A MATHEMATICAL MODELLING STUDY ON THE EFFECTS OF INTRACRANIAL AIR EXPANSION IN THE BRAIN ON THE INTRACRANIAL PRESSURE

VIRUJ BALA SOUPRAMANIEN

Supervisor: Dr. Ooi Ean Hin

A Thesis
submitted in partial fulfillment of the requirements for the
Degree in Bachelor of Engineering (Mechanical)
Faculty of Engineering
Monash University

October 2019

Certificate of Originality

I hereby declare that this submission is my own work and to the best of my knowledge it contains no materials previously published or written by another person, nor material which to a substantial extent has been accepted for the award of any other degree or diploma at Monash University or any other educational institution, except where due acknowledgement is made in the thesis. Any contribution made to the research by others, with whom I have worked at Monash University or elsewhere is explicitly acknowledged in the thesis.

I also declare that the intellectual content of this thesis is the product of my own work, except to the extent that assistance from others in the project's design and conception or in style, presentation and linguistic expression is acknowledged.

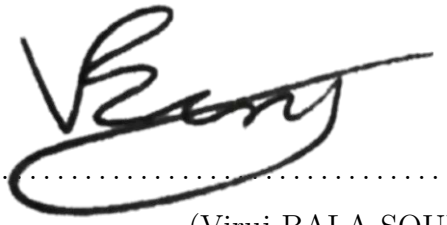

.....

(Viruj BALA SOUPRAMANIEN)

Acknowledgements

I want to thank my supervisor, Dr. Ooi Ean Hin, for his guidance through my final year project. I would also like to thank my parents who made it possible for me to go to university and for their support and help. I am also grateful for my brothers', Ravinash Gopauloo's and Neelesh Nursiah's aid throughout this project. The research discussed here was completed while at Monash University Malaysia.

Abstract

Pneumocephalus is a collection of air in the cranial cavity. Its presence can cause complications during air travel or post-surgery, altering intracranial pressure (ICP). The study presents a revision of the model proposed by Andersson et al. (2003). The effects of pneumocephalus on ICP during air travel and post-surgery are poorly understood. The proposed model first considered the absolute intracranial air pressure to depend on atmospheric pressure and ICP, and the simulation was solved numerically in MATLAB R2018b. The effects of varying ascension rates (exponential and logarithmic) on ICP were then investigated. Finally, the temperature effect on ICP post-craniotomy was explored. The proposed model simulated a maximum of 31% increase in intracranial air volume. The exponential function displayed a similar trend for intracranial volume but the ICP raised by larger increments. The logarithmic function showed a rise in ICP before dropping towards resting ICP near the maximum altitude (8000 ft). The temperature effects showed an increase of 8 mm Hg in ICP for a 6.3% intracranial air expansion (this was the worst-case scenario), taking 15 s. The proposed model represents more accurately the hydrodynamics of the intracranial system in the presence of pneumocephalus. The change in ICP was also found to be dependent on ascension rates and more so on rates of temperature change. The article provides findings of a revised model by Andersson et al. (2003), incorporating also the effects of varying ascension rates and the temperature effects on pneumocephalus and ICP.

Contents

List of Figures

List of Tables

List of Appendices

Chapter 1

Introduction

Intracranial pressure (ICP) is the measure of pressure inside the cranial cavity relative to ambient pressure. It is the pressure exerted on the intracranial contents; the cerebrospinal fluid (CSF), cerebral blood and brain parenchyma, inside the cranium. When there is a change in volume of one of the intracranial contents, the volumes of the other components will change accordingly to maintain a relatively constant cerebral volume, and thus keep intracranial pressure relatively constant. This is known as the Monroe-Kellie doctrine (Oswal and Toma 2017, Oddo and Le Roux 2010). Complications arising from head trauma, barotrauma, performing the Valsalva manoeuvre, or other head-related injuries may cause a change in cerebral volume and thus, a rise in ICP (Pishbin et al. 2015). This rise in ICP can be caused by the introduction of an intracranial mass lesion like pneumocephalus, a change in CSF circulation or the diffuse of intracranial pathological processes (Dunn 2002).

Pneumocephalus was first defined by Wolff (1914) as a collection of gas in the intracranial cavity. It may occur from traumatic (Lindvall and Bergenheim 2011) or non-traumatic (Pishbin et al. 2015) head injuries. It is a benign problem that is usually absorbed spontaneously (Sharma et al. 1989). Pneumocephalus can cause a mass effect on the brain, known as tension pneumocephalus (TP), should the rate of intracranial air continuously accumulate (Lindvall and Bergenheim 2011). Below 1500 mm Hg (200 kPa), air can be treated as an ideal gas and from the Boyle-Mariotte's law and Charles' law for ideal gas (Zemansky and Dittman 1997), when

there is a change in ambient pressure or temperature, volume of the gas will change accordingly. Also, according to Macmillan (1999) gas trapped in body cavities will expand when ambient pressure drops. Following this, in the presence of pneumocephalus, ICP is expected to increase should there be a fall in ambient pressure or a rise in ambient temperature.

One of the causes of pneumocephalus is from craniotomies. A craniotomy is a surgical process that involves surgery on the cranium. It is a complicated and critical process that, no matter however meticulously performed, may leave trace amounts of air in the skull (*Brain - Craniotomy* n.d., Mayfield n.d.). Owing to the rigidity of the skull, intracranial air cannot readily expand. This limitation in intracranial air expansion will result in the compression of one or more intracranial compartments thus, increasing ICP. Although pneumocephalus is not usually harmful, patients post-craniotomy are advised not to travel by air for a certain period. The timescales advised though, vary among surgeons, concerning air travel. It can range from less than two weeks to more than eight weeks (Amato-Watkins, Rao, and Leach 2013). There have been studies showing that in 85% of patients, intracranial air was absorbed within a week (Goldmann 1986). but others show it could be present up to three weeks (Reasoner et al. 1994).

Also, during a craniotomy, the patient's body temperature is cooled for the operation. The cold is used to suspend life, giving neurosurgeons time to complete the brain surgery. Performing this delicate operation using the cold is a powerful and puzzling technique that has the capability of bringing hope where there has been none before in the past [Fong 2010]. The surgery is performed by lowering body temperature in the range of 18-24°C. Once completed, patients are warmed to body temperature (∼37°C) using blankets or heating units. During this rise in temperature at constant ambient pressure, air trapped in body cavities will expand according to Charles' law for ideal gas. This increase in volume may cause the compression of the intracranial compartments, increasing ICP.

Several studies have been conducted to mathematically model the hydrodynamic relationships of the intracranial system (Andersson et al. 2003, Marmarou, Shulman, and Rosende 1978, Eklund et al. 2007, Lakin et al. 2003). Experimental studies use evasive techniques to monitor ICP, which themselves can alter ICP. Mathematical models offer an alternative, non-invasive method to study the intracranial system. However, the plausibility of such models are still being questioned and modified. Andersson et al. (2003) were the first to mathematically model the effects of pneumocephalus on the intracranial system. The findings of this model have been questioned in other studies (Donovan et al. 2008). There is also limited studies investigating the effects of pneumocephalus on the intracranial system during air travel. A thorough search of the relevant literature yielded no research that has investigated temperature effects on pneumocephalus and ICP either. This thesis will propose a revision of the model presented by Andersson et al. (2003) and incorporate the temperature effects on pneumocephalus and the intracranial system.

Chapter 2

Literature Review

Craniotomy is a complicated and critical process that involves surgery on the cranium. It is essential to repair fractures or ruptured vessels, remove large blood clots or tumours, or to relieve pressure on the brain. This process involves the surgical removal of a section of the skull to access the intracranial compartments. A craniotome (a special saw) is used to remove a bone flap granting access to the brain. Removing the bone flap exposes the dura matter, a protective membrane covering the brain. Small precise instruments are used to work deep inside the brain. After completing the operation, the dura matter is sewed shut and the bone flap is fixed back in place on the skull with plates and screws. During the replacement of the bone flap process, surgeons take extra care not to entrap air in the skull. Although, no matter how careful, this process often leaves traces of air trapped in the cranium (*Brain - Craniotomy* n.d., Mayfield n.d.). The trapped air is usually harmless and is spontaneously absorbed (Sharma et al. 1989). This phenomenon of gas collection in the cranial cavity is known as pneumocephalus (Wolff 1914).

There have been several clinical studies confirming the presence of intracranial air post-craniotomy. There have been reported cases of complications arising from intracranial air following air travel even in frequent air travels like pilots and soldiers (Canavan and Osborn 1991, Chan et al. 2000, Jensen and Adams 2004, Mirone et al. 2009, Javan et al. 2011, Huh 2013). The advised resting times after surgery and before air travel depends on surgeons. A survey conducted in the UK found

that the timescales ranged from less than 2 weeks to more than 8 weeks (Amato-Watkins, Rao, and Leach 2013). Experimental and theoretical studies have also provided different timescales for the lifespan of intracranial air (Seth et al. 2009, Ihab 2012, Brändström et al. 2017). Literature on pneumocephalus provide controversial findings. Goldmann (1986) found that intracranial air is absorbed within a week but from Reasoner et al. (1994) findings, pneumocephalus may be present up to 3 weeks post-craniotomy. In the Reasoner et al. (1994) study, 25% of patients were estimated to still have intracranial air and 11.8% of them have dangerous amounts of intracranial air even 3 weeks after surgery.

Shelesko, Chernikova, and Zaitsev (2017) reported only 8 clinical cases of spontaneous pneumocephalus from 1996 to 2016, portraying the rarity of this pathogen. The term "spontaneous pneumocephalus is used to describe intracranial air accumulation regardless of the cause. Pneumocephalus is normally caused by trauma to the head. Nonetheless, nontraumatic spontaneous pneumocephalus, from barotrauma, extracranial infections or by performing the Valsalva manoeuvres, is not uncommon (Pishbin et al. 2015). Spontaneous pneumocephalus is rare and accounts for only 0.6% of all pneumocephalus cases (Mirone et al. 2009). Since the etiological factors associated with pneumocephalus involve head injuries, surgical interventions and infections, and although being very rare, a defect in the cranial cavity will allow the development of spontaneous pneumocephalus (Shelesko, Chernikova, and Zaitsev 2017). Though, pneumocephalus is a benign complication, it can produce a mass effect on the brain should the rate of intracranial air accumulatoin continuously increase. This mass effect is known as tension pneumocephalus (TP) and may require surgery to relieve high pressure that could cause herniation (Lindvall and Bergenheim 2011). Air travel post-craniotomy can increase the risk of TP. Figures 2.1, 2.2 and 2.3 show computed tomography (CT) scans of a normal brain, one containing intracranial air and the effect of TP on the brain respectively.

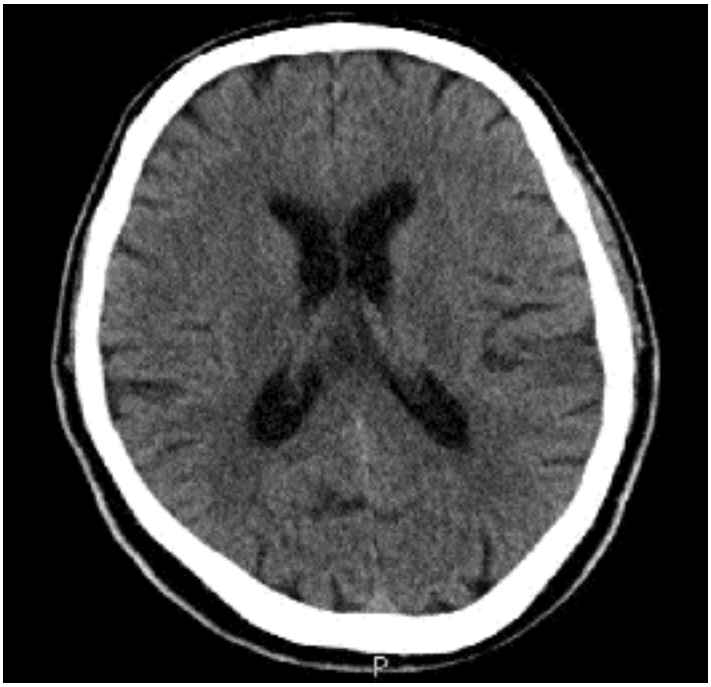

Figure 2.1: CT scan of brain with no abnormal lesion (Naqi and Azeemuddin 2013)

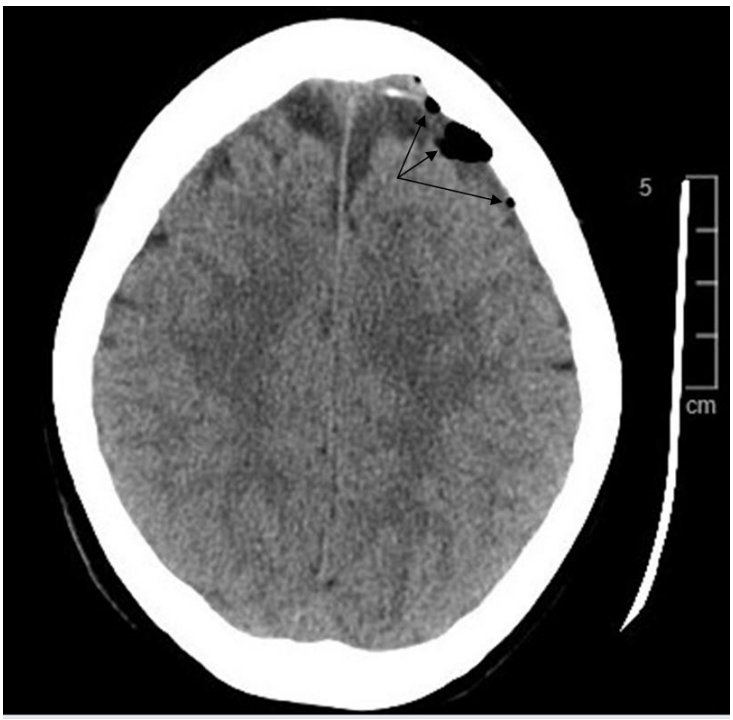

Figure 2.2: CT scan of brain with pneumocephalus, seen as black colour locules of air (Rashid et al. 2018)

Pneumocephalus patients may sometimes need aeromedical evacuation to undergo surgery to relieve pressure in the cranium. Air ambulance provides quick transport of patients requiring neurosurgical intervention, which can be critical.

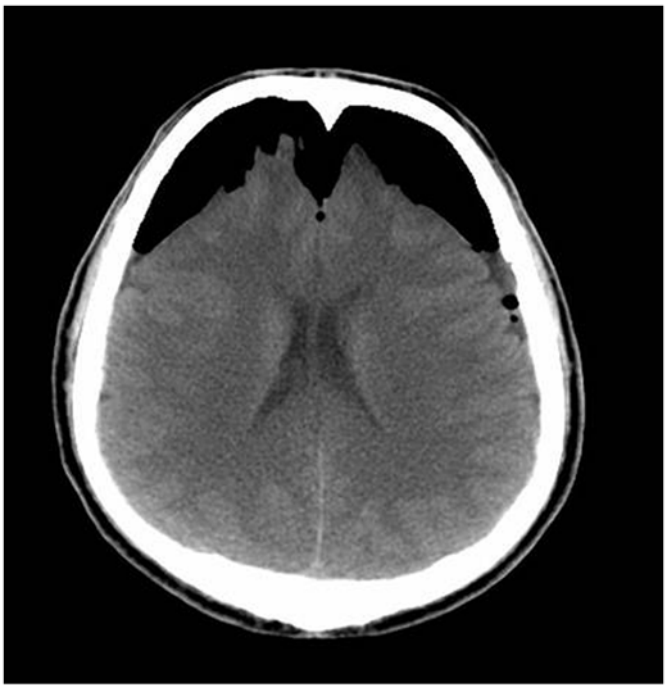

Figure 2.3: CT scan of brain with mass effect from pneumocephalus (Gokmen et al. 2015)

The safety of air travel for pneumocephalus patients is still a matter of debate due to the paucity and contradiction of relevant data (Seth et al. 2009, Amato-Watkins, Rao, and Leach 2013). Air ambulances therefore, pressurize cabins to approximately sea-level, usually 536-611 mm Hg (Huh 2013). Maintaining cabin pressure at such levels requires reducing the aircraft operational ceiling, 5000-8000 ft (Lindvall and Bergenheim 2011). At this lower altitude there is more turbulence and higher air resistance. The flight is less comfortable for the patients, more difficult for the pilot, the fuel consumption is increased, and the risk of a mishap is higher (Brändström et al. 2017). This is an expensive and technically demanding procedure (Seth et al. 2009). Although air ambulances can provide support to patients in need, there are reports of clinical deterioration during transport due to intracranial pathology (Lindvall and Bergenheim 2011).

Below pressures of 1500 mm Hg (200 kPa), air can be treated as an ideal gas (Zemansky and Dittman 1997). It has been established that gas trapped in body cavities will expand when there is a drop in ambient pressure (Macmillan 1999).

Due to the skull rigidity, intracranial air cannot expand readily. This limitation in intracranial air expansion will result in the compression of the brain thus, increasing ICP. The cerebral autoregulation can help in the management of ICP, but has its limits. The cerebral compliance is the final mechanism used to conntrol ICP changes. The Monro-Kellie hypothesis states that the intracranial volume is fixed. So the inclusion of any mass lesions occupying intracranial space, like pneumocephalus, will cause other intracranial compartments to accommodate for the change in intracranial volume.

According to the Monroe-Kellie doctrine, the contents of the skull are assumed to be constant and consist of the brain parenchyma (10%), cerebral blood (10%) and CSF (80%). When there is a change in volume in one of the cranial contents, the volumes of the other contents will change accordingly to maintain a relatively constant cerebral volume. Compensatory mechanisms are used to maintain a suitable and stable blood flow during changes in ICP, this is known as cerebral autoregulation (Oddo and Le Roux 2010, Oswal and Toma 2017). The compensatory mechanisms involve shifting of the CSF into the spinal compartment, increased absorption rate of CSF and displacement of cerebral blood into the venous sinuses(Savoy 1984).

If the cerebral autoregulation is impaired, i.e. when the compensatory reserves have been exhausted, a small change in intracranial volume will result in a steep increase in ICP. The volume-pressure relationship in the skull is non-linear which is quantified through the cerebral compliance. Altering intracranial compliance is the final mechanism for regulating ICP (Savoy 1984). Compliance is a physical property of tissue that describes the ability of a chamber to accommodate a change in its volume or pressure (Klabunde 2011). Compliance is considered to be a crucial characteristic of the cerebral hemodynamic. Alternative methods have been established to evaluate cerebral compliance (Portella et al. 2005). The Pressure Volume Index (PVI) proposed by Marmarou, Shulman, and Rosende (1978) is one of the most used techniques. PVI is the volume of CSF needed to raise the ICP ten-fold (Robertson et al. 1993).

Many studies have modelled the hydrodynamic relationships of the intracranial system for neurotrauma and hydrocephalus patients (Marmarou, Shulman, and Rosende 1978, Lakin et al. 2003, Eklund et al. 2007). Several studies considered the Monroe-Kellie hypothesis to describe the intracranial system (Marmarou, Shulman, and Rosende 1978, Eklund et al. 2007). However, the validity of these models have been questioned and modified in various aspects. Andersson et al. (2003) were the first to theoretically model the intracranial system to include pneumocephalus. During air travel when the atmospheric pressure drops, intracranial air volume will increase. Following the Monro-Kellie doctrine, the volumes of one or more of the other intracranial compartments will reduce to maintain normal ICP. Other than the cerebral autoregulation, cerebral compliance will also help adjust ICP.

There is some controversy regarding the effects of pneumocephalus on the intracranial system. For example, the studies of Goldmann (1986) and Reasoner et al. (1994) have contradicting findings. The survey conducted by Amato-Watkins, Rao, and Leach (2013) found that the timescales advised by neurosurgeons to travel by air post-craniotomy vary immensely. Peterson, Kent, and Cone (1944) found that in the absence of pneumocephalus, variations in ICP would be minimal, causing no concern. This goes against the findings of Kimoto et al. (2011) and Herbowski (2017). Donovan et al. (2008) have questioned the findings of Andersson et al. (2003). This paper offers a revision of the Andersson et al. (2003) model which came from the assumptions made in their study which will be further discussed.

Since air can be treated as an ideal gas, the model can be modified to include the effect of temperature on the system using Charles' law. During any operation, the operating theatre is cooled to lower the patient's body temperature. This is done to give surgeons enough time for the procedure. In the case of a craniotomy, patients' can be cooled to temperatures as low as 18°C (Fong 2010). After the procedure, patients are warmed back up to normal body temperature (37°C). This can cause an imbalance in the heat transfer from blood flow and the metabolic heat generation rate, inducing transient temperature changes (Rothmeier 2012). This change in

temperature will cause a change in intracranial air volume which will affect ICP to some extent. There have been studies modelling or investigating the mechanisms for hemodynamic cerebral activity-related temperature change (Rothmeier 2012). However, the effects of temperature on pneumocephalus and ICP is not known.

From the lack of evidence and contradiction of literature, there is much controversy on the effects of intracranial air on ICP. Temperature changes will also affect the change in air volume. A review of the literature provided no results concerning the impact of temperature on pneumocephalus and ICP. The proposed model will be designed to help shed some light on the contradictions and fill the paucity in the literature. This paper will provide a revised model of that proposed by Andersson et al. (2003). It will also investigate the effects of varying ascension rates on the intracranial system as well as incorporate the temperature effects on this system.

Chapter 3

Methodology

3.1 Mathematical Formulation of Intracranial System

The model proposed is a revision to that presented by Andersson et al. (2003). The schematics of the model proposed are shown in Figure 3.1. The system consists of the CSF, brain blood volume, brain tissue and the intracranial air. A state of hydrodynamic equilibrium is always assumed between the pressure and flow. The total inflow/expansion of the system (I_{tot}) is given by the sum of CSF formation rate (I_f) and expansion rate of intracranial air (I_{IA}). The model assumed the rates of re-absorption of air and fluid accumulation due to tissue swelling, to be negligible compared to I_f and I_{IA}. The outflow resistance R, dural sinus pressure P_d and ICP

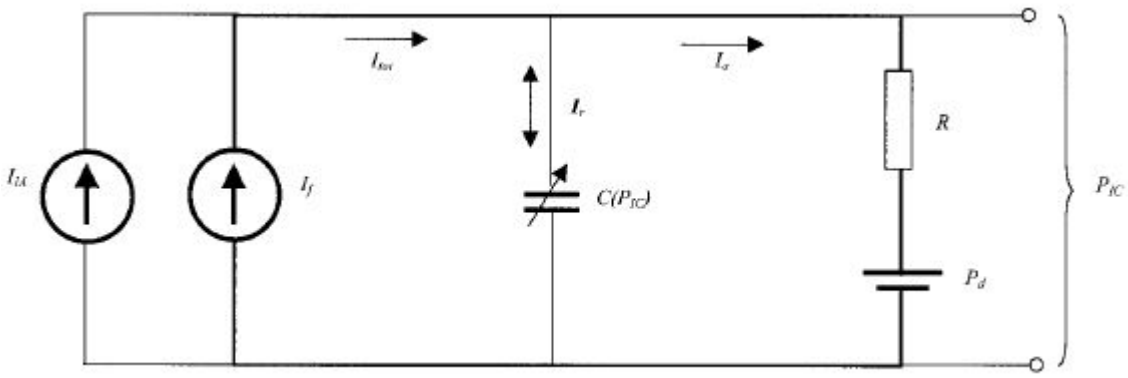

Figure 3.1: The analogous electrical system proposed by Andersson et al. (2003) which was an extension of that by Marmarou, Shulman, and Rosende (1978)

P_{IC} will influence the change in I_a, the CSF absorption rate into the venous blood. I_r is the part of the flow remaining in the system and is controlled by the cerebral compliance C, which is a function of ICP.

$$I_{tot} = I_{IA} + I_f = I_a + I_r \tag{3.1}$$

$$I_a = \frac{P_{IC} - P_d}{R} \tag{3.2}$$

The ICP governs the variation in intracranial compliance C, which will alter the brain blood volume and brain tissue compression. Compliance, as defined by Marmarou, Shulman, and Rosende (1978), is given by the ratio of change in cerebral blood volume to change in brain tissue pressure, and can also be determined from the volume-pressure curve of the system being studied. Cerebral compliance is thought to be an indication of the volume buffering capability of the brain (Portella et al. 2005).

$$C = \frac{dV_{IC}}{dP_{IC}} \tag{3.3}$$

The Pressure Volume Index (PVI) of Marmarou, Shulman, and Rosende (1978) can also be used to determine the mathematical expression for cerebral compliance. PVI is clinically defined as the volume of fluid (in millimetres) needed to raise the ICP ten-fold (Robertson et al. 1993). When assessed against a single individual, PVI can be assumed to be constant (Andersson et al. 2003).

$$PVI = \frac{P_{IC}}{0.4343}C \tag{3.4}$$

Due to the exponential nature of the intracranial volume-pressure relationship, cerebral compliance will decrease as ICP increases and can thus be expressed by the following expression (Marmarou, Shulman, and Rosende 1978):

$$C = \frac{1}{KP_{IC}} \tag{3.5}$$

The factor K is a mathematical expression where K = 1/(0.4343 PVI). It represents the steepness of the intracranial volume-pressure curve. From Equations 3.3 and 3.5, the time rate of ICP change is derived.

$$\frac{dP_{IC}}{dt} = \frac{dP_{IC}}{dV_{IC}}\frac{dV_{IC}}{dt} = KP_{IC}\frac{dV_{IC}}{dt} \tag{3.6}$$

The model considered the volume variation to occur only in the CSF, i.e., blood volume remains constant, then dV_{IC}/dt represents I_r. With this assumption and Equation 3.1, Equation 3.6 can be rewritten as:

$$\frac{dP_{IC}}{dt} = KP_{IC}I_r = KP_{IC}(I_{tot} - I_a) \tag{3.7}$$

Combining Equations 3.2 and 3.7 will set up the following differential equation:

$$\frac{dP_{IC}}{dt} + \frac{KP_{IC}^2}{R} - \frac{KP_{IC}}{R}(RI_{tot} + P_d) = 0 \tag{3.8}$$

When the rates of formation and absorption of CSF are in equilibrium, the system is in steady state. The pressure difference is dependent on I_f and R. P_d is thus, thought to regulate the steady state ICP (P_{IC_r}) on the ground at equilibrium ($P_{IC_r} = P_d + I_f R$). I_f, R and P_d can be assumed to be independent of ICP within the interesting pressure range and so were approximated as constants in the model (Gjerris and Børgesen 1992, Eide et al. 2001). Using this relationship and Equation 3.1, P_d and I_f can be removed from Equation 3.8 through:

$$RI_{tot} + P_d = R(I_f + I_{IA}) + P_{IC_r} - RI_f = RI_{IA} + P_{IC_r} \tag{3.9}$$

I_{IA} is the rate of change of intracranial air volume, dV_{IA}/dt. Using Equation 3.9, Equation 3.8 can be expressed as:

$$\frac{dP_{IC}}{dt} = \frac{KP_{IC}}{R}(R\frac{dV_{IA}}{dt} + P_{IC_r} - P_{IC}) \tag{3.10}$$

Andersson et al. (2003) solved Equation 3.10 using a linear approximation. The presented study simulated the results of this equation numerically using the ode45 solver in MATLAB R2018b.

3.2 Intracranial Air Expansion

3.2.1 Ambient Pressure Effect

In order to solve Equation 3.10, a relationship for V_{IA} (intracranial air volume) needs to be found first. This is achieved by taking advantage of the Boyle-Mariotte's law for ideal gas. The ideal gas law is given by $P_{IA}V_{IA} = n_{IA}R_uT_{IA}$, where R_u is the universal gas constant, P_{IA}, n_{IA} and T_{IA} represent the intracranial air pressure, number of moles and temperature respectively. Since T_{IA} and n_{IA} are also constants, V_{IA} can be expressed as:

$$V_{IA}(t) = \frac{V_{IA_0}P_{IA_0}}{P_{IA}(t)} \tag{3.11}$$

V_{IA_0} and P_{IA_0} are the initial intracranial volume and pressure respectively. P_{IA} was found to vary with atmospheric pressure (P_{atm}) and ICP, and thus, the following expression using the hydrostatic equation for the standard atmosphere can be derived (Andersson et al. 2003):

$$P_{IA}(t) = P_{atm}(t) + P_{IC}(t) = P_{atm_0}(1 - \alpha\frac{dH}{dt}t)^{\beta} + P_{IC}(t) \tag{3.12}$$

$\alpha = 2257 \times 10^{-}8$ and $\beta = 5.264$ are numerical constants, dH/dt is the rate of ascension, t is the time taken and P_{atm_0} is the atmospheric pressure at sea-level. P_{IA_0} is the initial intracranial air pressure at sea-level and can thus be approximated by P_{atm_0}. Andersson et al. (2003) neglected P_{IC} in Equation 3.12 approximating P_{IA} to

P_{atm} because of the magnitude of atmospheric pressure compared to ICP. However, this assumption suggests that ICP is a constant when in fact it is continuously varying. Thus, this model investigated the influence of ICP also on P_{IA}. Then combining Equations 3.11 and 3.12, and differentiating with respect to time will yield:

$$\frac{dV_{IA}}{dt} = \frac{V_{IA_0}P_{atm_0}}{(P_{atm_0}(1-\alpha\frac{dH}{dt}t)^{\beta} + P_{IC}(t))^2}(\alpha\beta P_{atm_0}(\frac{dH}{dt} + \frac{d^2H}{dt^2}t)(1-\alpha\frac{dH}{dt}t)^{\beta-1} + \frac{dP_{IC}}{dt}) \tag{3.13}$$

Equation 3.13 is inserted into Equation 3.10 and is solved numerically in MATLAB to find the change in ICP with change in altitude.

3.2.2 Ambient Temperature Effect

To evaluate the effect of temperature on V_{IA}, Charles' law for ideal gas is used. From the ideal gas equation, $P_{IA}V_{IA} = n_{IA}R_uT_{IA}$, P_{IA} is considered a constant instead of T_{IA} and so V_{IA} can be expressed as a function of T_{IA}.

$$V_{IA}(t) = \frac{V_{IA_0}}{T_i}T_{IA}(t) \tag{3.14}$$

T_i is the initial body temperature right after surgery, before the patient is warmed. Since the intracranial air is enclosed within the cranial cavity, its temperature is expected to vary with the body temperature, T. So, T_{IA} is approximated by T. Equation 3.14 is differentiated, to set up the following equation:

$$\frac{dV_{IA}}{dt} = \frac{V_{IA_0}}{T_i}\frac{dT}{dt} \tag{3.15}$$

dT/dt is the rate of temperature change to reach 37°C. Equation 3.15 is inserted into Equation 3.10 and is solved numerically in MATLAB to evaluate the change in ICP as a function of temperature.

3.3 Parameter Selection

Table 3.1: Parameter selection for model

Parameter	Value	Unit
P_{IC_r}	10 and 20	mm Hg
PVI	12.6	ml
R	16.1	mm Hg·ml^{-1}·min^{-1}
V_{IA_0}	10, 20 and 30	ml
dH/dt	250, 500 and 1000	ft·min^{-1}
X	2288, 2824 and 3641	ft
Y	141.49, 223.04 and 375.23	ft
Z	0.0015, 0.0026 and 0.0042	min^{-1}
T_i	18, 21 and 24	°C
dT/dt*	2.99 ± 0.4, 1.95 ± 0.3 and 1.05 ± 0.2	K·s^{-1}

* Temperature change rate depends on initial intracranial air volumes and temperatures. See Table 3.2

The parameters used in the model are shown in Table 3.1. All ICP simulations were done for 10 mm Hg (normal P_{IC_r}) 20 mm Hg (high P_{IC_r}). The worst-

case scenarios were chosen and so PVI was assumed to be 12.6 ml and 16.1 mm Hg·ml^{-1}·min^{-1} for R. The amount of intracranial air present was estimated at volumes 10, 20 and 30 ml to cover a considerable scope. To study the effect of dH/dt, constant ascension rates of 250, 500 and 1000 ft·min^{-1} were assumed. For varying ascension rates, two additional cases were analyzed:

- A logarithmic change in altitude:

$$H = Xln(t+1) \rightarrow \frac{dH}{dt} = \frac{X}{t+1} \rightarrow \frac{d^2H}{dt^2} = -\frac{X}{(t+1)^2} \tag{3.16}$$

- An exponential change in altitude:

$$H = Ye^{Zt-1} \rightarrow \frac{dH}{dt} = YZe^{Zt-1} \rightarrow \frac{d^2H}{dt^2} = YZ^2e^{Zt-1} \tag{3.17}$$

H is the change in altitude. X, Y and Z are numerical constants that were evaluated. The model simulated results until a maximum altitude of 8000 ft for all dH/dt. X, Y and Z were estimated so that the exponential and logarithmic functions took the same amount of time as the constant ascension rates to reach 8000 ft, as shown in Figure 3.2.

For the temperature effect, the time rate of temperature change, dT/dt, was needed. A patient's body temperature is usually lowered during an operation depending on the nature of the surgery (Fong 2010). So this study investigated the effects of three different initial temperatures, T_i (18, 21 and 24°C), as shown in Table 3.1, on pneumocephalus and the intracranial system. The results were simulated

using dT/dt to reach 37°C. However, dT/dt depended on T_i and the V_{IA_0}. A simulation was conducted in COMSOL Multiphysics Simulation Software to estimate the time taken to warm a patient from T_i to 37°C (Rothmeier 2012, Nour et al. 2015). Table 3.2 shows the time rate of change of these initial temperatures to reach 37°C for all V_{IA_0}. dT/dt was found by evaluating the gradient of the temperature-time graphs to reach 37°C from T_i. Figure 3.3 shows the temperature-time curve for all three initial intracranial air volumes.

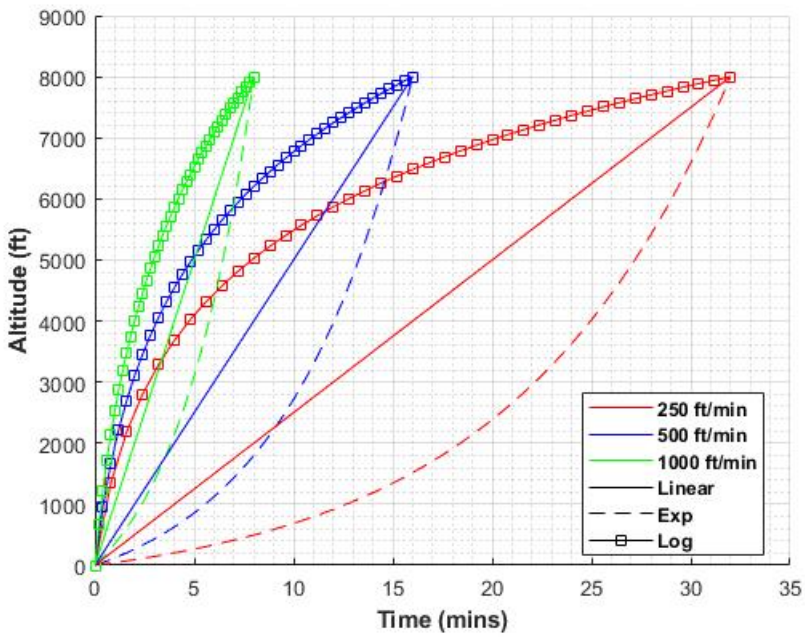

Figure 3.2: Linear, logarithmic and exponential functions of altitude with time

Table 3.2: Time rate of temperature change (K·s^{-1}) for three initial temperatures and volumes

V_{IA_0} (ml) \ T_i (°C)	18	21	24
10	3.54	2.97	2.45
20	2.32	1.95	1.58
30	1.25	1.05	0.85

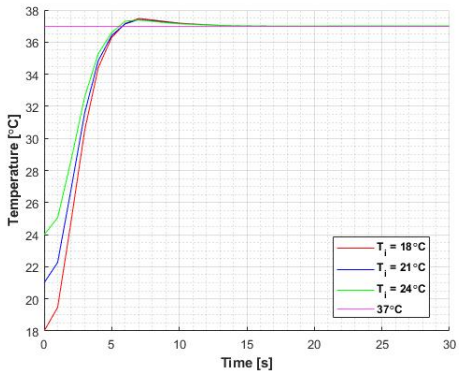

(a) 10 ml

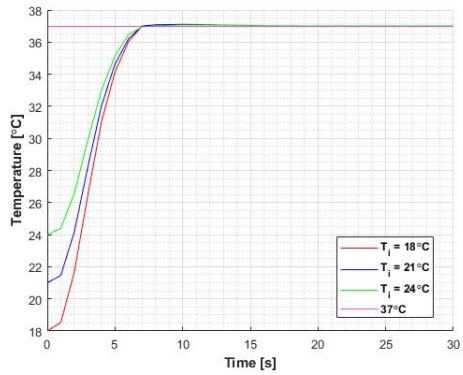

(b) 20 ml

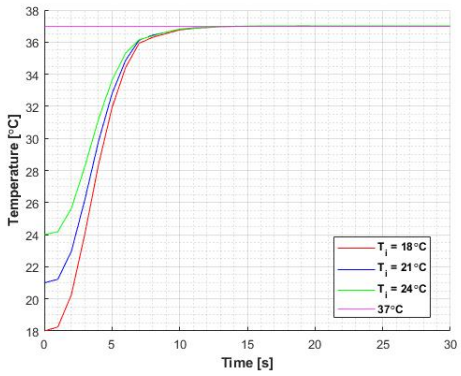

(c) 30 ml

Figure 3.3: Temperature change against time for all initial volumes

Chapter 4

Results

4.1 Change in Ambient Pressure

This section presents the results for ascension rates corresponding to 500 ft·min^{-1}. Simulated results for ascension rates corresponding to 250 and 1000 ft·min^{-1} are provided in Appendix A.1 and A.2. The results of this section were plotted with that obtained from Andersson et al. (2003) for comparison.

4.1.1 Constant Ascension Rates

The results were simulated in MATLAB using the constant ascension rates and the other parameters from Table 3.1. These parameters and Equations 3.11 and 3.13 were used to simulate the effects of altitude change on the intracranial air volume (Figure 4.1) and the rate of change of intracranial air volume (Figure 4.2). Each figure show curves for the three initial volumes until a maximum height of 8000 ft was reached. In the Andersson et al. (2003) model, intracranial air volume increased by almost 35% whereas the proposed model found that the volume would increase by 31%.

Using Equations 3.10 and 3.13, and parameters from Table 3.1, change in ICP was found as a function of altitude for 10 and 20 mm Hg resting pressures (Figure 4.3). For higher initial volumes, resting pressure and ascension rates, the change in ICP was higher. This is expected with normal cerebral autoregulation. The change in ICP of the proposed model was lower than that found by Andersson et al. (2003). Also, the difference between the two models grew for higher initial volumes and resting pressures as can be seen from Figure 4.3.

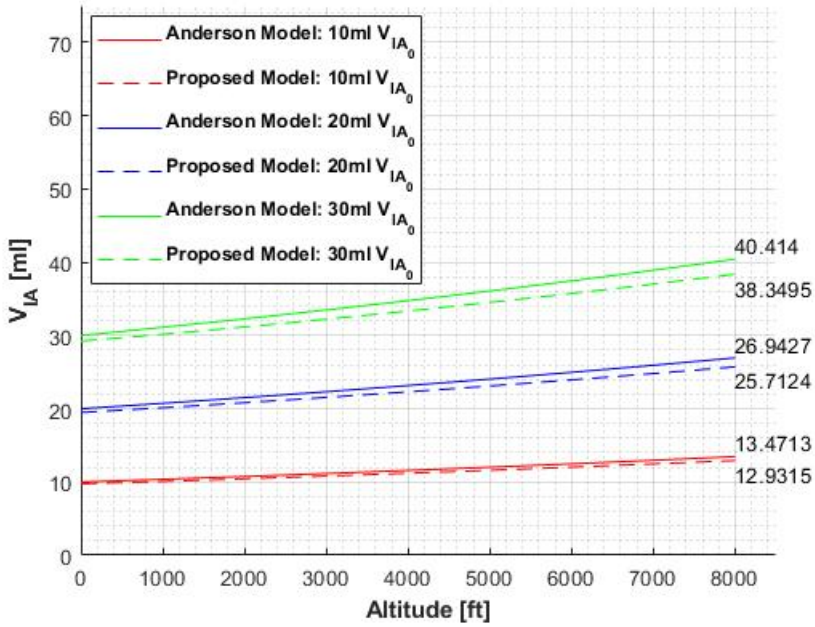

Figure 4.1: Change in intracranial air volume during ascent at 500 ft·min^{-1}, simulated for three initial volumes

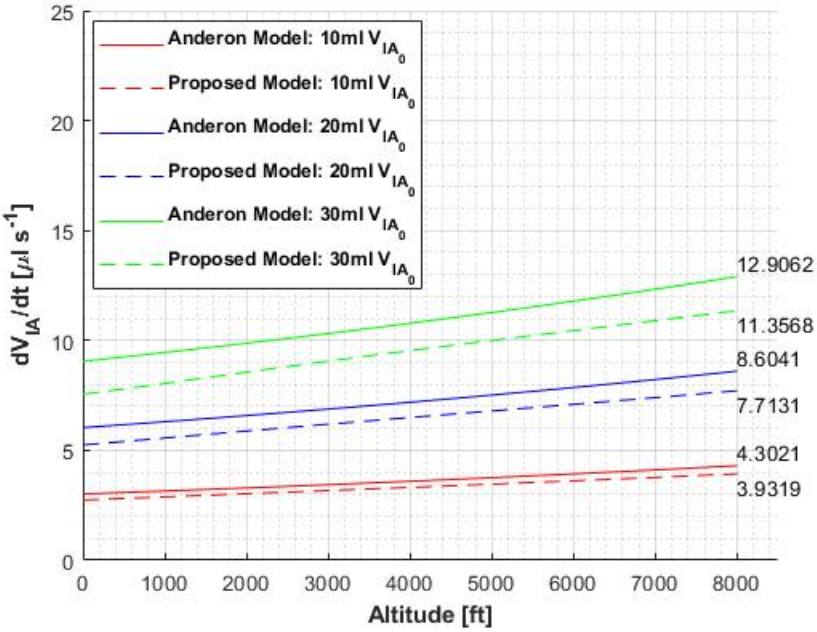

Figure 4.2: Rate of change of intracranial air volume during ascent at 500 ft·min^{-1}, simulated for three initial volumes

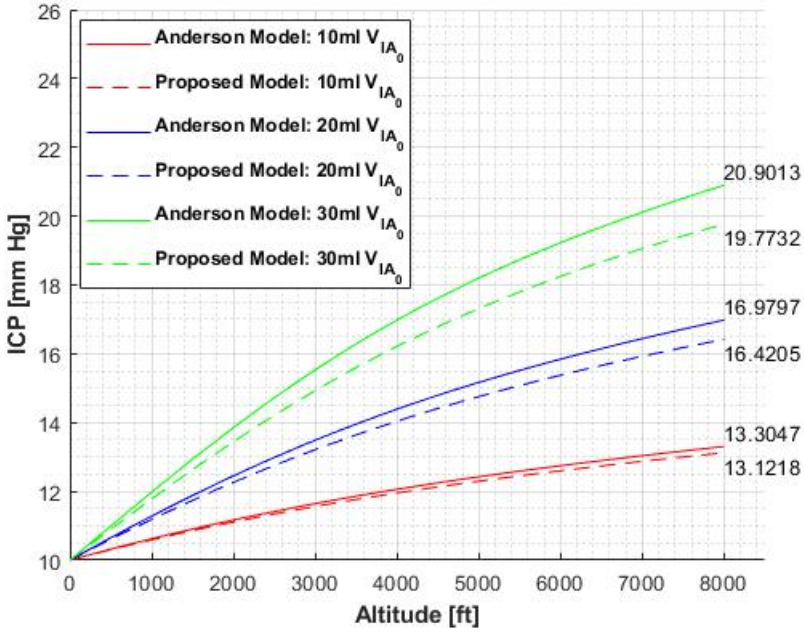

(a) 10 mm Hg

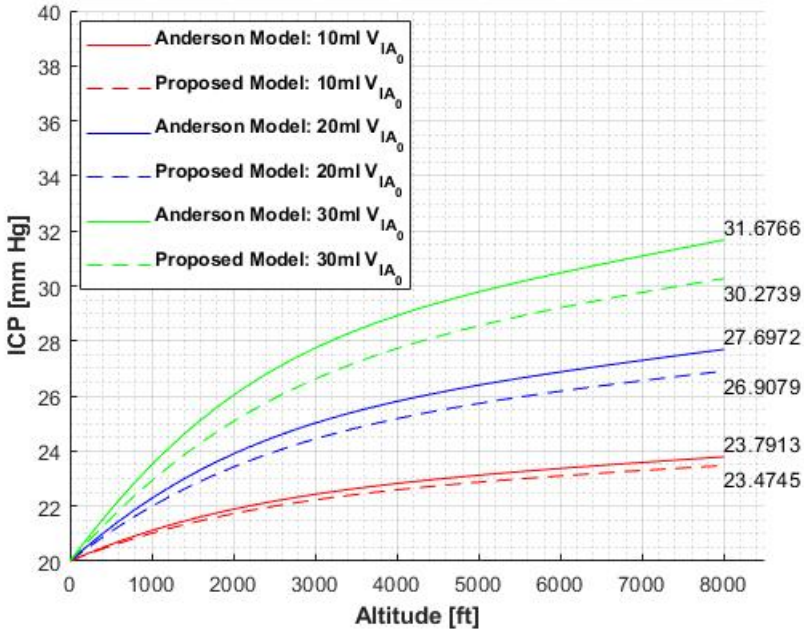

(b) 20 mm Hg

Figure 4.3: Change in ICP during ascent at 500 ft·min^{-1}, simulated for three initial volumes and two resting ICP

4.1.2 Varying Ascension Rates

To investigate the effects of varying ascension rates on the intracranial system, Equations 3.10, 3.11 and 3.13, and values from Table 3.1 were used. Equation 3.16 was used to simulate results for a logarithmic ascension and Equation 3.17 for an exponential ascension. The results from Andersson et al. (2003) were also simulated for comparison. This section presents the results corresponding to 500 ft·min^{-1} rate of altitude changes. The simulated results corresponding to ascension rates of 250 and 1000 ft·min^{-1} are presented in Appendix A.2.

Logarithmic Ascension

Using Equation 3.16 to simulate the effects of a logarithmic ascension on intracranial air volume, rate of change of intracranial air and ICP, are presented in Figures 4.4, 4.5 and 4.6 respectively. These figures used the ascension rate that corresponded to 500 ft·min^{-1}, i.e. the value of X was 2824 ($H = 2824\ln(t + 1)$), which took 16 mins to reach 8000 ft. Intracranial air volume (Figure 4.4) increased by 1.5% compared to a 4.5% increase with the Andersson et al. (2003) model. The rate of change of intracranial air (Figure 4.5) decreased to 0 at around 3000 ft regardless of the initial air volume, however, with higher initial volumes, rate of change of intracranial air was found to decrease faster. Figure 4.6 shows the change in ICP for both resting pressures. Again there was a difference between Andersson et al. (2003) and the proposed model which became more significant for higher initial volumes. Interestingly, after around 3000 ft, both model showed a decrease in ICP towards the resting pressure.

Exponential Ascension

The effects of an exponential ascension on the intracranial system were simulated using Equation 3.17. Figures 4.7, 4.8 and 4.9 show the change in intracranial air volume, rate of change of intracranial air and change in ICP respectively as functions of altitude. The model behaved as expected owing to the nature of the exponential function. Again the difference between Andersson et al. (2003) and the proposed model was more significant as initial volume increased. The function that produced these curves corresponded to 500 ft·min^{-1}, i.e. it took 16 mins to reach 8000 ft (H = $223.04e^{0.0026t-1}$). Similar to the constant ascension rate (Chapter 4.1.1), using Andersson et al. (2003) model, intracranial volume increased by 35% and the proposed model simulated an increase of nearly 30% in intracranial air volume.

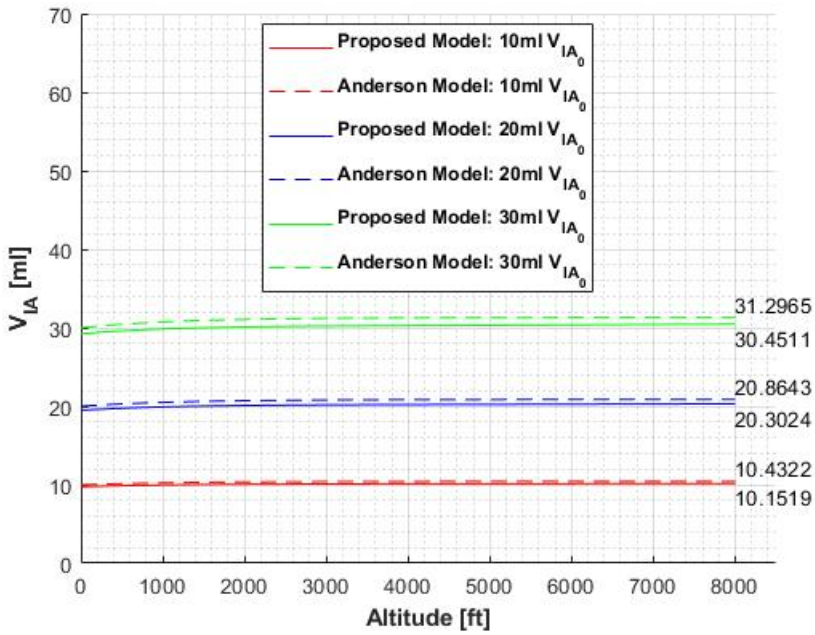

Figure 4.4: Change in intracranial volume during logarithmic ascension simulated with three initial volumes

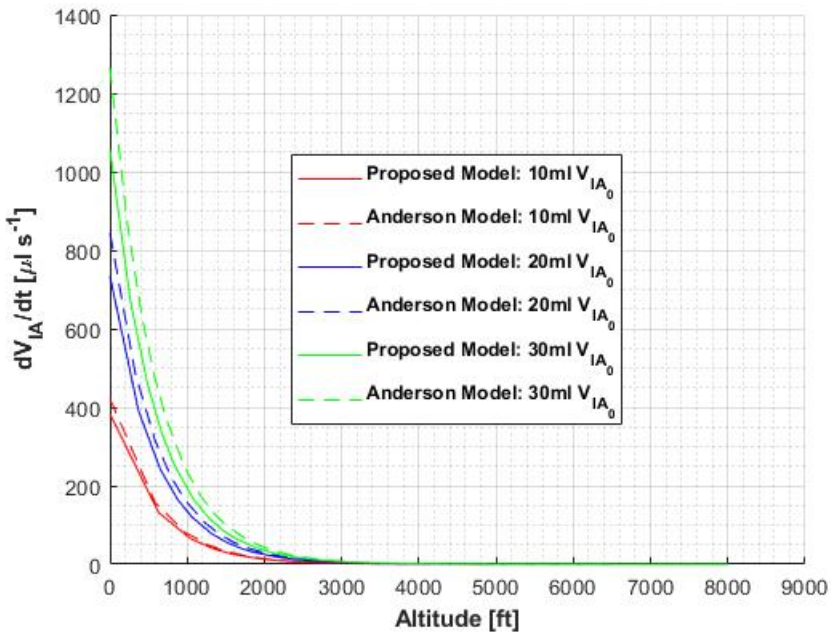

Figure 4.5: Rate of change of intracranial volume during logarithmic ascension simulated with three initial volumes

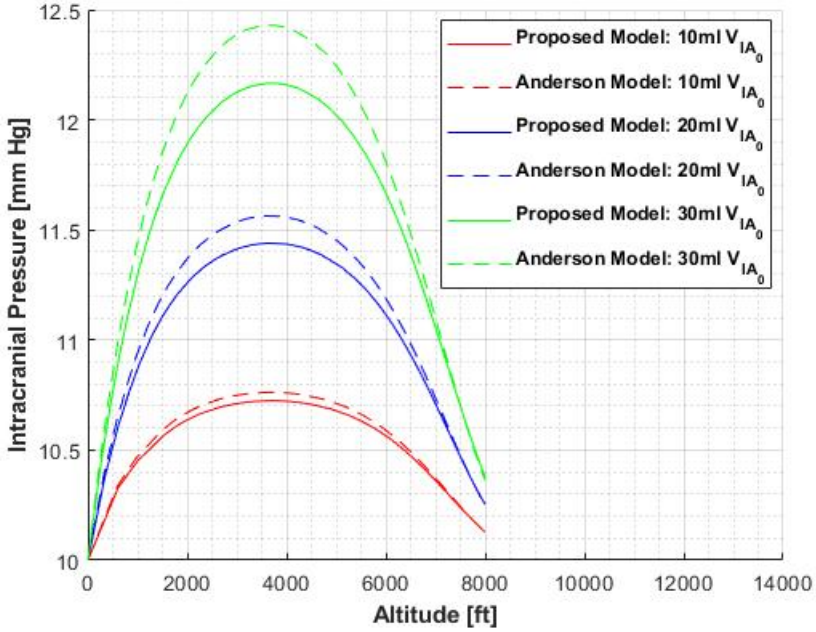

(a) 10 mm Hg

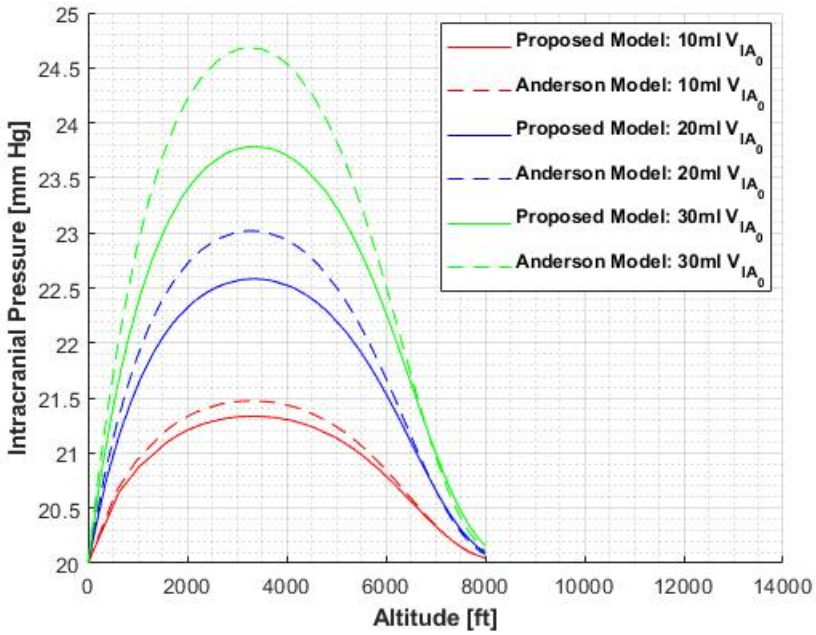

(b) 20 mm Hg

Figure 4.6: Change in ICP during logarithmic ascension with three initial volumes and two resting pressures

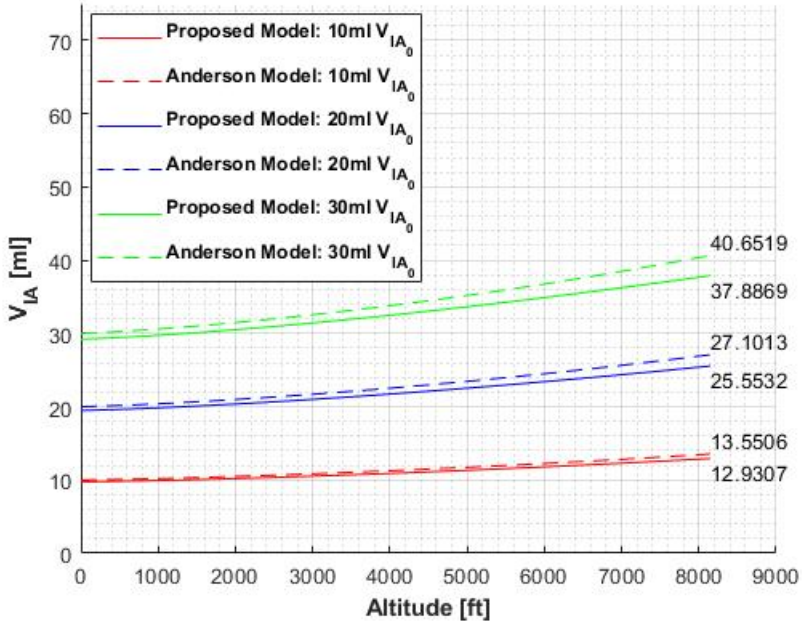

Figure 4.7: Change in intracranial volume during exponential ascension simulated with three initial volumes

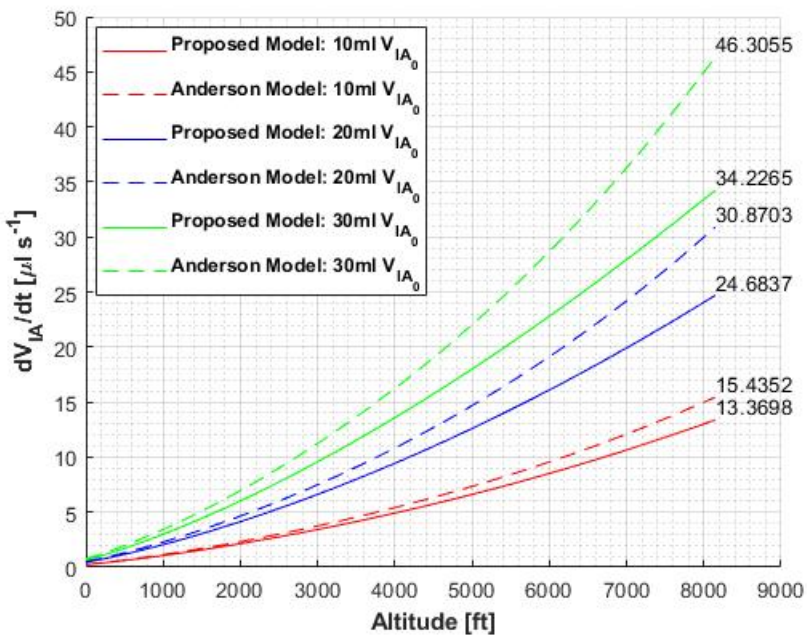

Figure 4.8: Rate of change of intracranial volume during exponential ascension simulated with three initial volumes

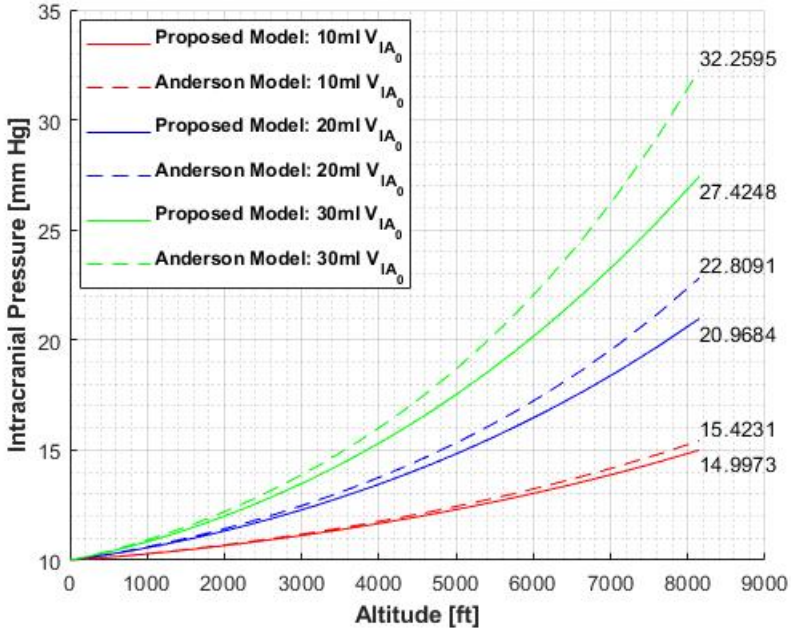

(a) 10 mm Hg

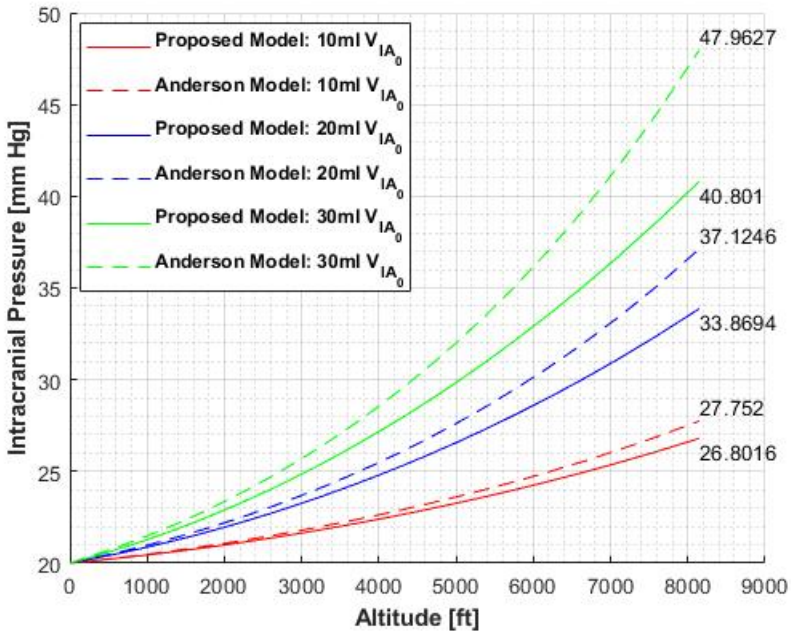

(b) 20 mm Hg

Figure 4.9: Change in ICP during exponential ascension with three initial volumes and two resting pressures

4.2 Change in Ambient Temperature

Equations 3.10 and 3.15, and values in Tables 3.1 and 3.2 were used to simulate the effects of temperature on the intracranial system. Figure 4.10 shows the change in intracranial air volume with temperature for the three initial volumes for 18, 21 and 24°C initial temperatures. The model simulated, for the worst-case scenario (T_i = 18°C and V_{IA_0} = 30 ml, green line in Figure 4.10(a)), an increase of 6.3% in intracranial air volume. This corresponded to an increase in ICP by 4.5 mm Hg when resting pressure was 10 mm Hg and 8 mm Hg for 20 mm Hg resting pressure (Figure 4.11). The best-case scenario in this simulation would be when T_i = 24°C and V_{IA_0} = 10 ml (red line in Figure 4.10(c)). A 4.1% expansion in intracranial air caused a 0.78 mm Hg increase in ICP for 10 mm Hg resting pressure, which again was almost double for 20 mm Hg resting pressure. Figures 4.11, 4.12 and 4.13 show the change in ICP with temperature for 18, 21 and 24°C initial temperatures.

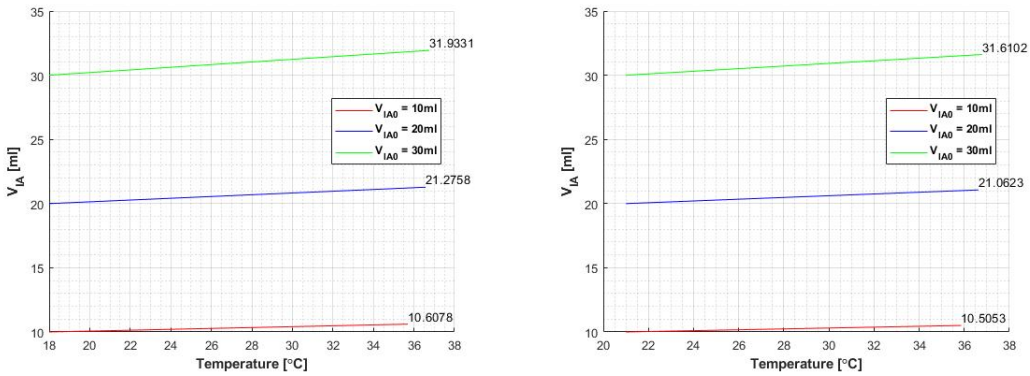

(a) 18°C

(b) 21°C

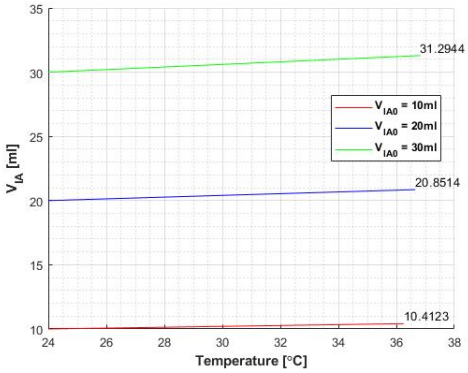

(c) 24°C

Figure 4.10: Change in intracranial volume with change in temperature simulated with three initial volumes and initial temperatures

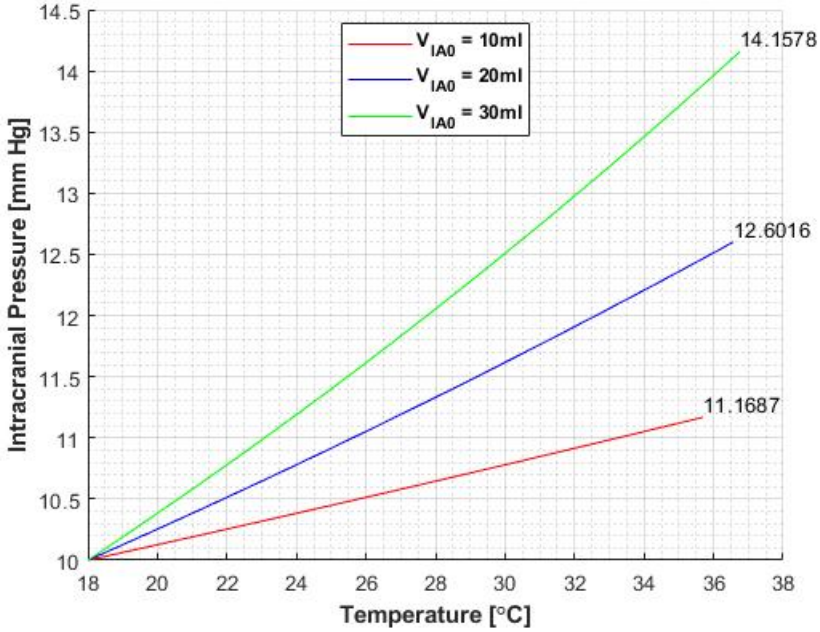

(a) 10 mm Hg

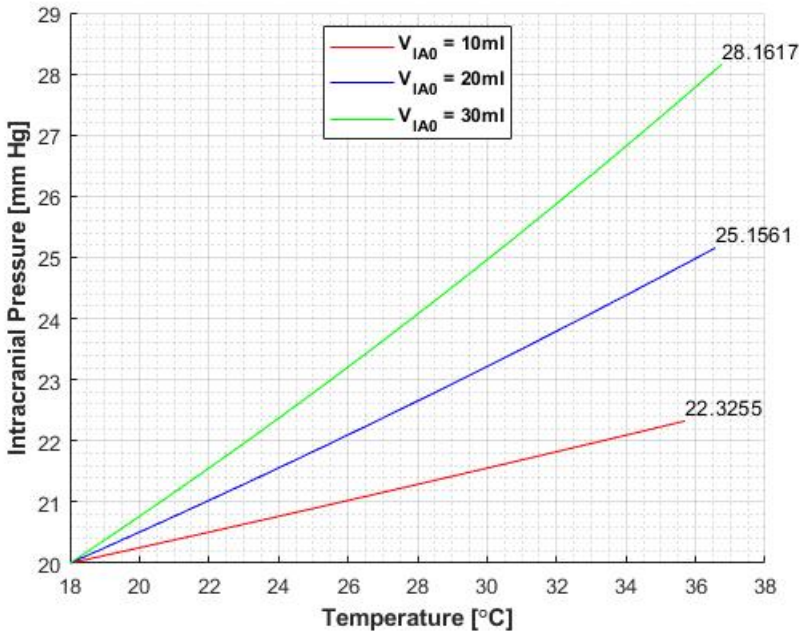

(b) 20 mm Hg

Figure 4.11: Change in ICP with temperature simulated with three initial volumes, two resting pressures and 18 °C initial temperature

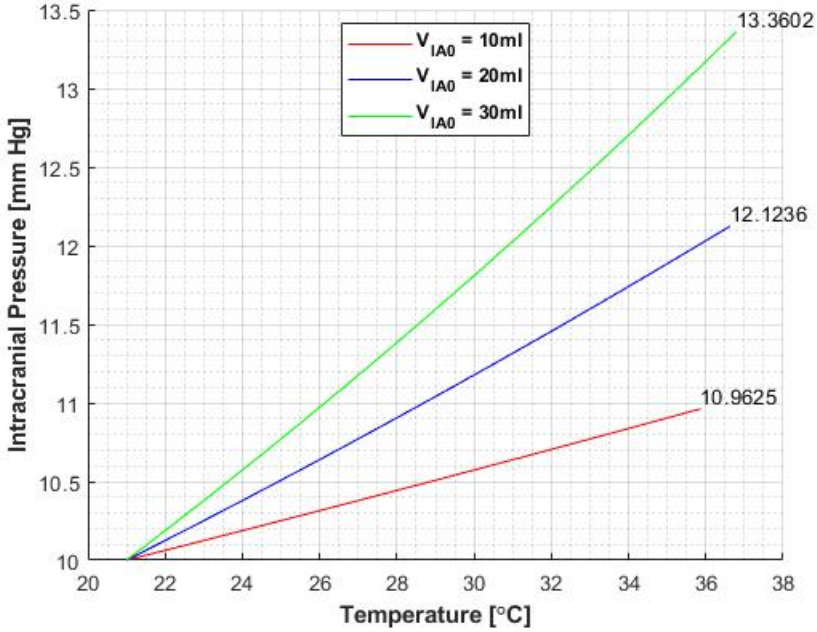

(a) 10 mm Hg

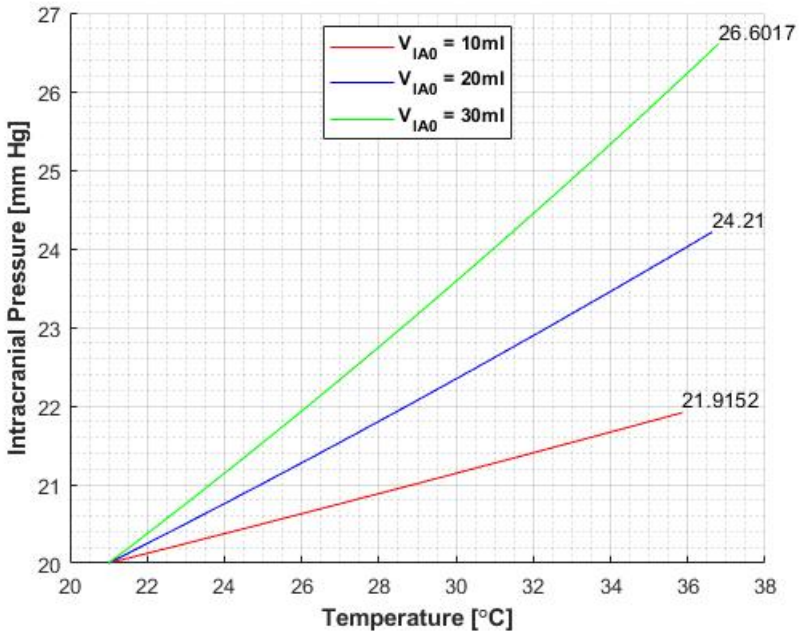

(b) 20 mm Hg

Figure 4.12: Change in ICP with temperature simulated with three initial volumes, two resting pressures and 21 °C initial temperature

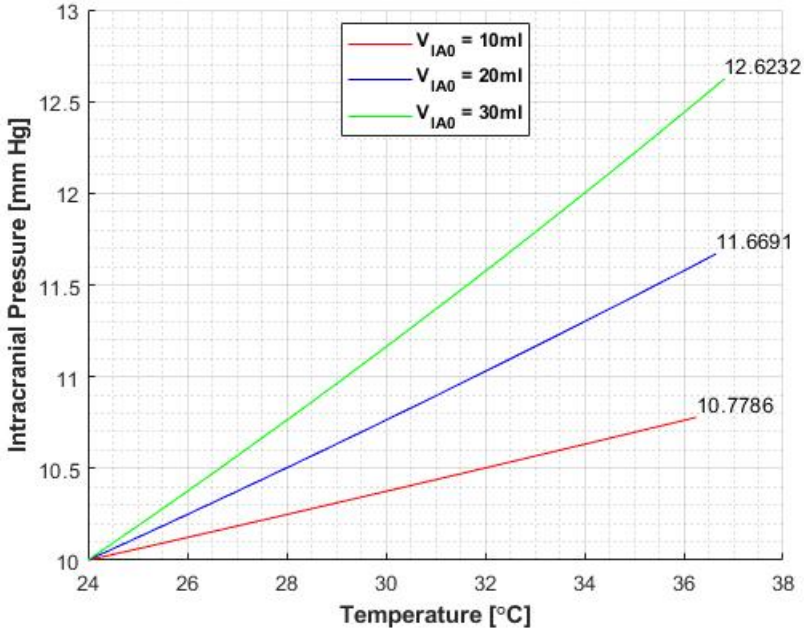

(a) 10 mm Hg

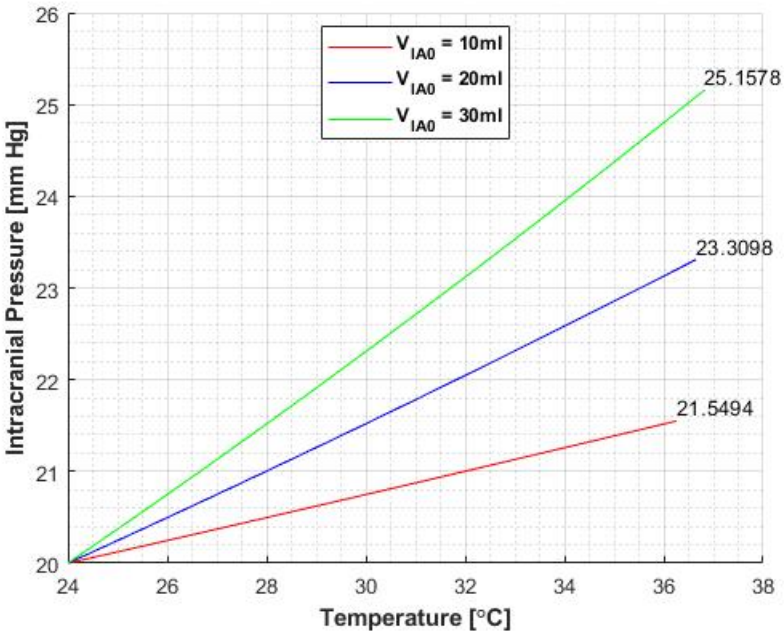

(b) 20 mm Hg

Figure 4.13: Change in ICP with temperature simulated with three initial volumes, two resting pressures and 24 °C initial temperature

Chapter 5

Discussion

5.1 Validity of Model

The effects concerning altitude change in ICP, in the presence of pneumocephalus, had not been previously explored before Andersson et al. (2003). There has been a previous study, conducted by Lincoff, Weinberger, and Stergiu (1989) on the influence of intraocular gas on the intraocular pressure during air travel. The motivation of this study arose from reports of pain and vision loss during ascension, and it was found that the presence of gas caused intraocular pressure to increase as ambient pressure fell. In the results of the simulations presented (Chapter 4.1.1), the change in ICP is dependent on the initial intracranial air volumes and temperatures, and ascension rates. The fluid mechanics of the eye and brain are similar and so, can be hydrodynamically characterised by the outflow resistance R, CSF production rate I_f, and cerebral compliance C (Aronowitz and Brubaker 1976). This supports the findings of the calculations.

Andersson et al. (2003) had based their study on Marmarou, Shulman, and Rosende (1978), as they were among the first to introduce the exponential nature of the volume-pressure relationship. Although the Marmarou, Shulman, and Rosende (1978) model has been debated and updated in several ways, it is well recognized and documented and so was selected as the basis of the Andersson et al. (2003)

model. The Marmarou, Shulman, and Rosende (1978) model determines ICP following the injection of synthetic CSF into the system. In the simulations presented in this paper, the change in volume was caused by the expansion of pneumocephalus. Whether it is the blood, CSF or intracranial air that induced the change in volume would not impact the system's pressure-volume relationship. Therefore the relationships applicable for artificial infusion will still be relevant in these scenarios, and the use of previous models of the system is supported. From Equation 3.13, $V_{IA}(t)$ clearly depends on dH/dt and Equation 3.14 shows the dependence of $V_{IA}(t)$ on T(t). The hydrodynamic system works in such a way that the spatial compensation of the intracranial air, depends on the rate of of change of ambient pressure or the rate of change of ambient temperature (Avezaat and Van Eijndhoven 1986).

ICP remains relatively stable during change in ambient pressure and temperature in the absence of pneumocephalus. Peterson, Kent, and Cone (1944) conducted a case study of a human subject. During simulated ascents to altitudes of 49,000-59,000 ft at 0.55-1.64 ft·min^{-1} ascension rates, it was found that there was no change in ICP. The influence of pneumocephalus though, affects these conditions. It has been established that gas trapped in bodily orifices will expand as ambient pressure decreases (Macmillan 1999). Due to compliance and since atmospheric pressure is applied uniformly to the entire body, intracranial air can expand to some degree. Thus, intracranial air assumes absolute pressure (Equation 3.12).

5.2 Comparison with Andersson et al. (2003) Model

The assumptions made for this model were as follows. The air bubble trapped in the cranial cavity was assumed to be a sphere, and so, the increase in volume was uniform. For pressures below 1500 mm Hg (200 kPa), air can be treated as an ideal gas (Zemansky and Dittman (1997)). The Boyle-Mariotte's law can thus, be used

to describe the volume-pressure relationship during air travel, and Charles' law for the volume-temperature relationship post-craniotomy. From CT scans, it has been noticed that the location of pneumocephalus depends on the position of the patient (Schirmer, Heilman, and Bhardwaj 2010) and since large pressure gradients are not expected in the brain, intracranial air will expand similarly irrespective of the intracranial air location and geometry (Andersson et al. 2003).

The proposed model numerically solved the differential equation (Equation 3.10) instead of using a linear approximation to simulate the results. Also, it was found that the intracranial air pressure varies with ambient pressure and ICP. However, the Andersson et al. (2003) study assumed ICP to be constant in this relationship (Equation 3.12) and due to the difference in magnitude, approximated Equation 3.12 by atmospheric pressure. However, it has been found that ICP is a varying parameter that depends on the cerebral compliance C, mean arterial pressure (MAP) and cerebral perfusion pressure (CPP) (Portella et al. 2005). The proposed model provided slightly improved results compared to the Andersson et al. (2003) model. The difference in ICP between the two models (where the proposed model simulated results of lower magnitudes compared to the Andersson et al. (2003) model) became more significant as initial air volumes, resting pressures and ascension rates increased as seen from the Figure 4.3 and the results presented in Appendix A.1.

5.3 Varying Ascension Rates

Although the altitude is an important factor, it is the rate of altitude change that is more crucial. Andersson et al. (2003) investigated only the effects of constant ascension rates on the intracranial system including pneumocephalus (Chapter 4.1.1). After a revision of their model, the study investigated the effects of accelerating and decelerating ascension rates. This was done by analyzing exponential and log-

arithmic (Chapter 4.1.2 and Appendix A.2) ascensions. These two ascension rates (Equations 3.16 and 3.17) were simulated in the Andersson et al. (2003) and proposed models, and the results were compared.

5.3.1 Exponential Ascension

To study accelerating ascension rates, an exponential function was used to describe the change in altitude over time. Thus, Equation 3.17 was derived such that the parameters Y and Z allowed the function to reach the altitude of 8000 ft in 32, 16 and 8 mins which correspond to the constant ascension rates 250, 500 and 1000 ft·min^{-1} respectively, to reach this altitude. From the relevant parameters in Table 3.1, and Equations 3.10, 3.13 and 3.17, the effects of an exponential ascension on pneumocephalus and ICP were simulated.

The results obtained from the simulation, presented in Chapter 4.1.2 and Appendix A.2.2, were similar to that for constant ascension rates (Chapter 4.1.1 and Appendix A.1). There was no change in the results from the Andersson et al. (2003) model for change in intracranial air volume. The proposed model simulated a 30% increase in air volume compared to 31% with the constant ascension rates (Figure 4.7). ICP increased by greater magnitudes with the exponential ascension than constant ascension rates for both models, although the intracranial air expansions were similar. This supports the fact that change in ICP is influenced greatly by the ascension rate (Jensen and Adams 2004). Also, similarly to the constant ascension rates, for higher initial air volumes and resting pressure, ICP will reach higher levels and the difference between the two models becomes more significant.

5.3.2 Logarithmic Ascension

During a logarithmic ascension, the rate of altitude change is decreasing over time during the ascension. Equation 3.16 describes the logarithmic ascension used in the simulation. The parameter X was found such that the Equation 3.16 reaches 8000 ft in 32, 16 and 8 mins corresponding to the times taken for the constant ascension rates (250, 500 and 1000 ft·min^{-1}) to reach this altitude. Using parameters from Table 3.1, and Equations 3.10, 3.13 and 3.16, the effects of logarithmic ascension on pneumocephalus and ICP were simulated.

It was found that intracranial air increased by 4.5% in volume using Andersson et al. (2003) model compared to a 1.5% increase in the proposed model (Figure 4.4). This expansion caused a rise in ICP until 3000-4000 ft, after which ICP dropped back to resting pressure (Figure 4.6). Since the ascension rate using the logarithmic function is decreasing, until the altitude of 8000 ft is reached, the timeframe for spatial compensation to reduce net volume is larger (Avezaat and Van Eijndhoven 1986) compared to the linear and exponential ascensions. From Figure 4.5, it can be seen that the intracranial air expansion rate decreases until 3000 ft after which it stops. Thus, ICP levels have time to decrease to resting pressure before the altitude of 8000 ft is reached. Since aircrafts would follow similar ascension rates to the logarithmic function, the fall in ICP after a certain height could explain why some pneumocephalus patients experience minor or no complications during air travel.

Furthermore, from the results in Chapter 4.1.2 and Appendix A.2.1, higher ICP levels are reached for higher initial volumes, resting pressures and ascension rates. Again the dependence of ICP on the ascension is highlighted by these results (Chapter 4.1.2) compared with those obtained for linear and exponential ascensions. With the logarithmic ascensions, the maximum ICP level reached was the lowest of the three ascension rate cases.

5.4 Temperature Effect

The temperature dynamics of brain tissue are governed by the balance of the metabolic heat generation rate and heat transfer with blood supply across capillaries contained in the brain tissue, nearby tissues and the surroundings. Upsetting this balance will cause transient temperature changes (Rothmeier 2012). The model included transient temperature change by making use of Charles' law to obtain the volume-temperature relationship. Using COMSOL Multiphysics Simulation Software, the time taken for intracranial air temperature to increase from initial to normal body temperature (37°C) were found. The temperature-time curves (Figure 3.3) obtained from these simulations were used to find the time rate of temperature change shown in Table 3.2. Parameters of Tables 3.1 and 3.2, and Equations 3.10 and 3.15 were used to simulate the effects of temperature change on the intracranial system containing pneumocephalus.

5.4.1 Results

The results for the temperature simulations are presented in Chapter 4.2. From Figure 4.10, it was noticed that for lower initial temperatures, the intracranial air expansion was greater. Also, similar with the change in ambient pressure effects (Chapter 4.1), higher initial air volumes caused greater change in intracranial air expansion. For the worst-case scenario (the green line in Figure 4.10(a)), the 6.3% increase in intracranial air volume caused ICP to increase by 4.5 mm Hg when resting pressure was 10 mm Hg, which almost doubled for 20 mm Hg resting pressure (Figure 4.11). The change in ICP was greatest when initial temperature was lowest. Also, as initial air volumes increased and for higher resting pressures, the change in ICP was larger.

5.4.2 Comparison with Pressure Effects

In Chapter 4.1, it was found that the change in ICP was highly influenced by the rate of altitude change. For constant ascension rates, an increase of 31% in air volume caused ICP to increase by about 10 mm Hg (Figure 4.3). For exponential ascension the 30% intracranial air expansion saw an increase of almost 20 mm Hg in ICP (Figure 4.9). When logarithmic ascension was considered, the 1.5% increase in air volume saw a 2.2-3.8 mm Hg increase in ICP depending on the resting pressure (Figure 4.6). Compared to the ICP simulations presented in Chapter 4.2, it would seem that the temperature change has a greater impact on the ICP than the pressure change. However, it should be noted that for the worst-case scenario, the time taken to reach normal body temperature (37°C) was approximately 10-15 s and the best-case scenario was 5-6 s, whereas the ambient pressure effects occurred over the span of 32, 16 or 8 mins depending on the ascension rate.

5.5 General Discussion

This study, like that of Andersson et al. (2003), is limited to normal aircraft conditions. However, on top of providing an improved version of their model, this study did take into account the effects of accelerating and decelerating ascension rates on the intracranial system. The results of these simulations proved the dependence of ICP on the rates of altitude change, where higher rates caused greater increase in ICP. From the temperature effects it was found that the rate of temperature change had a greater impact on ICP than the ascension rates. Moreover, for higher initial volumes and resting pressures as well as lower initial temperatures, ICP can reach high levels. The difference between the Andersson et al. (2003) and proposed models increased for higher initial air volumes and resting pressures, in the case of changing ambient pressure.

Results in Chapter 4.1.2 and Appendix A.2.1 suggest that ICP would decrease back to resting pressure before the cruising altitude is reached (8000 ft in this paper). There have been reports of patients experiencing complications only during ascent and landing. Some of these patients were hospitalized after days, weeks or months due to effects of pneumocephalus following air travel (Chan et al. 2000, Jensen and Adams 2004, Javan et al. 2011). The findings of these papers could be explained by the change in the ICP for logarithmic ascension. Yet, since these patients needed medical treatment after a certain period after travelling, further examination of the model would be needed to provide a definitive explanation.

The model however, does provide an overestimate. This is because the model assumes equilibrium with the pressure or temperature inside the intracranial air and that of the surroundings. This means the air can expand without resistance until similar ambient conditions are met. In reality the skull would resist the indefinite intracranial air expansion along with the brain compliance. The next step would be to include the skull rigidity. Also, the CPP and MAP could be incorporated in the model to provide a more accurate change in ICP. The CPP is also known to have a significant influence on the cerebral vascular resistance and blood volume which regulate the constant blood flow (Portella et al. 2005). As for the temperature effect, instead of using COMSOL to simulate the change in temperature, the temperature distribution in the brain, CPP, MAP and metabolic heat generation could be implemented in the model to investigate its influence on ICP (Nour et al. 2015, Rothmeier 2012). The temperature effect during ascension could also be investigated to include in the model. With rising altitudes, ambient temperature and pressure will decrease (McCullough and Fox 1974, Filippidis et al. 2011). From the results, decreasing ambient pressure and lower initial temperature cause a change in ICP.

Chapter 6

Conclusion

Following the assumptions made by Andersson et al. (2003), this paper presents a revision of their model of the hydrodynamics of the intracranial system including pneumocephalus. In the proposed model, Equation 3.10 was solved numerically in MATLAB using the ode45 solver instead of using a linear approximation to simulate the change in ICP. Also, it is known that ICP is not constant and varies in response to various stimuli. Thus, the intracranial air pressure, which has been said to vary with ICP and atmospheric pressure, was not approximated by atmospheric pressure only (Equation 3.12). It was also found that difference between the two models became more significant for higher initial intracranial air volume and resting pressure (Chapter 4.1.1).

Andersson et al. (2003) investigated the effects of constant ascension rates in their study. This research was extended to aircrafts of varying ascension rates. Two additional cases were analyzed on top of constant ascension rates: accelerating and decelerating rates of altitude change. This was achieved by simulating the effects of exponential and logarithmic ascensions on pneumocephalus and ICP. The results from Chapter 4.1.2 prove the dependence of ICP on the rate of altitude change. For faster ascensions, ICP was found to reach much higher levels compared to lower ascension rates. Moreover, with the logarithmic ascension, the ICP fell back to resting pressure after a certain altitude was reached. Since aircrafts would normally

follow a similar flight profile, it could explain why some pneumocephalus patients experience little to no complications during air travel.

This paper also presented the findings of the temperature effect on the intracranial system containing pneumocephalus (Chapter 4.2), which had not been previously explored. The change in temperature of the intracranial air varied with initial air volumes and temperatures. For lower initial temperatures the change in ICP was larger. Compared to the change in ambient pressure (Chapter 4.1), it seemed that the rate of temperature change had a greater effect on ICP than the rate of altitude change. The timescale for the temperature effect was shorter than pressure changes, suggesting that the time rate of change is highly important in influencing ICP changes. The timeframe for spatial compensation to reduce net volume is a significant factor when monitoring ICP.

To sum up, this paper provides a revision of the model proposed by Andersson et al. (2003). The effects of varying ascension rates and temperature changes on the intracranial system were also investigated. The model describes the hydrodynamic relationships of the intracranial system incorporating pneumocephalus. The model's behaviour agrees with physical expectations and the simulated results depict the dependence of ICP on the rate of altitude change and more so on the rate of temperature change. For high initial air volumes, high resting pressures and low initial air temperatures, ICP may reach high levels. Further examination of the model would provide useful insight for neurosurgeons and responders of aeromedical evacuation, to ensure pneumocephalus patients' comfort and to avoid serious complications.

Bibliography

Amato-Watkins, Anthony, Veeru Mudigunda Rao, and Paul Leach (2013). "Air travel after intracranial surgery: a survey of advice given to patients by consultant neurosurgeons in the UK". In: *British journal of neurosurgery* 27.1, pp. 9–11.

Andersson, Nina et al. (2003). "Air transport of patients with intracranial air: computer model of pressure effects". In: *Aviation, space, and environmental medicine* 74.2, pp. 138–144.

Aronowitz, Jerome D and Richard F Brubaker (1976). "Effect of intraocular gas on intraocular pressure". In: *Archives of Ophthalmology* 94.7, pp. 1191–1196.

Avezaat, CJJ and JHM Van Eijndhoven (1986). "Clinical observations on the relationship between cerebrospinal fluid pulse pressure and intracranial pressure". In: *Acta neurochirurgica* 79.1, pp. 13–29.

Brain - Craniotomy (n.d.). URL: https://www.goodmancampbell.com/brain-craniotomy.

Brändström, Helge et al. (2017). "Risk for intracranial pressure increase related to enclosed air in post-craniotomy patients during air ambulance transport: a retrospective cohort study with simulation". In: *Scandinavian journal of trauma, resuscitation and emergency medicine* 25.1, p. 50.

Canavan, L and RE Osborn (1991). "Dural sinus air without head trauma or surgery: CT demonstration." In: *Journal of computer assisted tomography* 15.3, p. 526.

Chan, Yun P et al. (2000). "Acute confusion secondary to pneumocephalus in an elderly patient." In: *Age and ageing* 29.4, pp. 365–367.

Donovan, Daniel J et al. (2008). "Aeromedical evacuation of patients with pneumocephalus: outcomes in 21 cases". In: *Aviation, space, and environmental medicine* 79.1, pp. 30–35.

Dunn, Laurence T (2002). "RAISED INTRACRANIAL PRESSURE". In: *Journal of Neurology, Neurosurgery & Psychiatry* 73.suppl 1, pp. i23–i27. ISSN: 0022-3050. DOI: 10.1136/jnnp.73.suppl_1.i23. eprint: https://jnnp.bmj.com/content/73/suppl_1/i23.full.pdf. URL: https://jnnp.bmj.com/content/73/suppl_1/i23.

Eide, Per et al. (2001). "Assessment of intracranial pressure volume relationships in childhood: the lumbar infusion test versus intracranial pressure monitoring". In: *Child's Nervous System* 17.7, pp. 382–390.

Eklund, Anders et al. (2007). "Assessment of cerebrospinal fluid outflow resistance". In: *Medical & biological engineering & computing* 45.8, pp. 719–735.

Filippidis, Aristotelis S et al. (2011). "Negative-pressure and low-pressure hydrocephalus: the role of cerebrospinal fluid leaks resulting from surgical approaches to the cranial base: Report of 3 cases". In: *Journal of neurosurgery* 115.5, pp. 1031–1037.

Fong, Dr Kevin (Sept. 2010). *Surgeons use cold to suspend life*. URL: https://www.bbc.com/news/health-11389464.

Gjerris, F and SE Børgesen (1992). "Current concepts of measurement of cerebrospinal fluid absorption and biomechanics of hydrocephalus". In: *Advances and technical standards in neurosurgery*. Springer, pp. 145–177.

Gokmen, IE et al. (2015). "Mount Fuji sign following surgical drainage of spinal epidural abscess". In: *QJM: An International Journal of Medicine* 108.10, pp. 835–836.

Goldmann, Robert W (1986). "Pneumocephalus as a consequence of barotrauma". In: *Jama* 255.22, pp. 3154–3156.

Herbowski, Leszek (2017). "The major influence of the atmosphere on intracranial pressure: an observational study". In: *International journal of biometeorology* 61.1, pp. 181–188.

Huh, Jisoon (2013). "Barotrauma-induced pneumocephalus experienced by a high risk patient after commercial air travel". In: *Journal of Korean Neurosurgical Society* 54.2, p. 142.

Ihab, Zidan (2012). "Pneumocephalus after surgical evacuation of chronic subdural hematoma: Is it a serious complication?" In: *Asian journal of neurosurgery* 7.2, p. 66.

Javan, Ramin et al. (2011). "Spontaneous pneumocephalus after commercial air travel complicated by meningitis". In: *Aviation, space, and environmental medicine* 82.12, pp. 1153–1156.

Jensen, Matt B and Harold P Adams (2004). "Pneumocephalus after air travel". In: *Neurology* 63.2, pp. 400–401.

Kimoto, Kazuhito et al. (2011). "Influence of barometric pressure in patients with migraine headache". In: *Internal Medicine* 50.18, pp. 1923–1928.

Klabunde, Richard E. (2011). *Compliance*. URL: https://www.cvphysiology.com/Cardiac%20Function/CF013.

Lakin, William D et al. (2003). "A whole-body mathematical model for intracranial pressure dynamics". In: *Journal of mathematical biology* 46.4, pp. 347–383.

Lincoff, Harvey, Dov Weinberger, and Panos Stergiu (1989). "Air travel with intraocular gas: II. Clinical considerations". In: *Archives of Ophthalmology* 107.6, pp. 907–910.

Lindvall, Peter and Tommy Bergenheim (2011). "Air Transportation of Patients with Brain Tumours". In: *Tumors of the Central Nervous system, Volume 3*. Springer, pp. 339–343.

Macmillan, Alistair JF (1999). "The effects of pressure change on body cavities containing gas". In: *Aviation Medicine. 3rd ed. Oxford, UK: Reed Educational and Professional Publishing Ltd*, pp. 13–19.

Marmarou, Anthony, Kenneth Shulman, and Roberto M Rosende (1978). "A nonlinear analysis of the cerebrospinal fluid system and intracranial pressure dynamics". In: *Journal of neurosurgery* 48.3, pp. 332–344.

Mayfield (n.d.). *Craniotomy, Craniectomy: Mayfield Brain Spine, Cincinati, OH*. URL: https://mayfieldclinic.com/pe-craniotomy.htm.

McCullough, David C and John L Fox (1974). "Negative intracranial pressure hydrocephalus in adults with shunts and its relationship to the production of subdural hematoma". In: *Journal of neurosurgery* 40.3, pp. 372–375.

Mirone, G et al. (2009). "Spontaneous intraparenchymal tension pneumocephalus triggered by compulsive forceful nose blowing". In: *Emergency Medicine Journal* 26.11, pp. 837–838.

Naqi, Rohana and Muhammad Azeemuddin (2013). "Naeglaeria infection of the central nervous system, CT scan findings: a case series". In: *J Pak Med Assoc* 63.3, pp. 399–402.

Nour, Mhamed et al. (2015). "3D Simulation of the Laser Interstitial Thermal Therapy in Treatment (LITT) of Brain Tumors". In: *Proceedings of the 2015 COMSOL Conference in Boston*, pp. 1–6.

Oddo, Mauro and Peter Le Roux (2010). "57 What Are the Etiology, Pathogenesis, and Pathophysiology of Elevated Intracranial Pressure?" In: *Evidence-Based Practice of Critical Care E-book: Expert Consult: Online and Print*, p. 399.

Oswal, Ashwini and Ahmed K Toma (2017). "Intracranial pressure and cerebral haemodynamics". In: *Anaesthesia & Intensive Care Medicine* 18.5, pp. 259–263.

Peterson, Eric W, Basil S Kent, and William V Cone (1944). "Intracranial pressure in the human subject at altitude". In: *Archives of Neurology & Psychiatry* 52.6, pp. 520–525.

Pishbin, Elham et al. (2015). "Spontaneous nontraumatic pneumocephalus: A case report". In: *Iranian Red Crescent Medical Journal* 17.7.

Portella, G et al. (2005). "Continuous cerebral compliance monitoring in severe head injury: its relationship with intracranial pressure and cerebral perfusion pressure". In: *Acta neurochirurgica* 147.7, pp. 707–713.

Rashid, Murtaza et al. (2018). "Pneumocephalus after Epidural Anesthesia". In: *British Journal of Medical Practitioners* 11.2, pp. 10–12.

Reasoner, Daniel K et al. (1994). "The incidence of pneumocephalus after supratentorial craniotomy. Observations on the disappearance of intracranial air." In: *Anesthesiology* 80.5, pp. 1008–1012.

Robertson, CS et al. (1993). "Intracranial Compliance and Cerebral Hemodynamics in Head-Injured Patients". In: *Intracranial Pressure VIII*. Springer, pp. 535–539.

Rothmeier, Greggory H (2012). "Brain tissue temperature dynamics during functional activity and possibilities for optical measurement techniques". In:

Savoy, Suzanne M (1984). "The craniotomy patient. Identifying the patient's neurological status." In: *AORN journal* 40.5, pp. 716–724.

Schirmer, Clemens M., Carl B. Heilman, and Anish Bhardwaj (Aug. 2010). "Pneumocephalus: Case Illustrations and Review". In: *Neurocritical Care* 13.1, pp. 152–158. ISSN: 1556-0961. DOI: 10.1007/s12028-010-9363-0. URL: https://doi.org/10.1007/s12028-010-9363-0.

Seth, R et al. (2009). "Fitness to fly post craniotomy–a survey of medical advice from long-haul airline carriers". In: *British journal of neurosurgery* 23.2, pp. 184–187.

Sharma, Bhawani Shanker et al. (1989). "Tension pneumocephalus following evacuation of chronic subdural haematoma". In: *British journal of neurosurgery* 3.3, pp. 381–387.

Shelesko, EV, NA Chernikova, and OS Zaitsev (2017). "A rare case of spontaneous pneumocephalus as a complication of nontraumatic nasal liquorrhea". In: *J Clin Case Rep* 7.1012, p. 2.

Wolff, E (1914). "Air accumulation in the right lateral ventricle of the brain (pneumocephalus)". In: *Munch Med Wochenschr* 61, p. 899.

Zemansky, M and R Dittman (1997). *Heat and Thermodynamics. McGraww-Hill Inc.*

Nomenclature

α	Numerical constant
β	Numerical constant
C	Cerebral compliance
CPP	Cerebral perfusion pressure
CSF	Cerebrospinal fluid
CT	Computed tomography
dH/dt	Rate of change of altitude
dT/dt	Rate of change of temperature
H	Altitude
I_a	CSF absorption rate into venous blood
I_f	CSF production rate
I_r	Flow of fluid remaining in the system
I_{IA}	Rate of intracranial air expansion
I_{tot}	Total fluid flow rate in system
ICP, P_{IC}	Intracranial pressure
K	Mathematical constant
MAP	Mean arterial pressure
P_d	Dural sinus pressure

P_{atm}	Atmospheric pressure
P_{IA}	Intracranial air pressure
P_{atm_0}	Atmospheric pressure at sea level
P_{IA_0}	Initial intracranial air pressure
P_{IC_r}	Resting intracranial pressure
PVI	Pressure volume index
R	Outflow resistance of system
T	Body temperature
t	Time taken
T_i	Initial body temperature
T_{IA}	Intracranial air temperature
TP	Tension pneumocephalus
V_{IA}	Intracranial air volume
V_{IC}	Volume of intracranial system
V_{IA_0}	Initial intracranial air volume

Appendices

Appendix A

Simulated Results

A.1 Constant Ascension Rates

Simulated results for constant ascension rates are presented here.

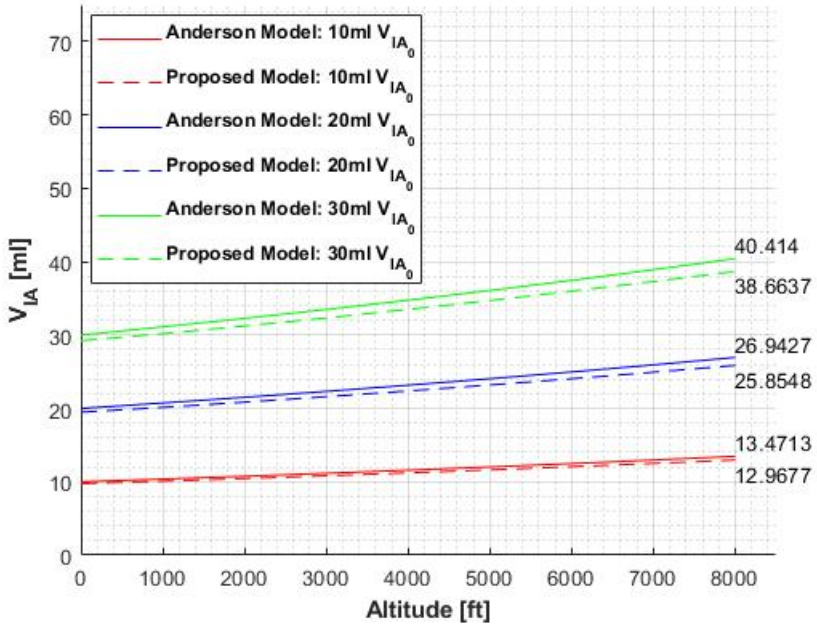

Figure A.1: Change in intracranial air volume during ascent at 250 ft·min^1, simulated for three initial volumes

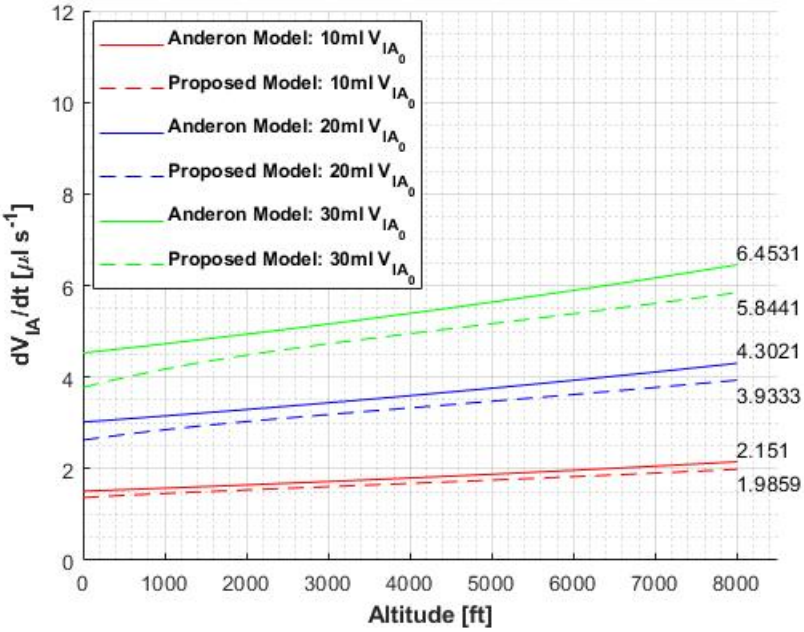

Figure A.2: Rate of change of intracranial air volume during ascent at 250 ft·min^1, simulated for three initial volumes

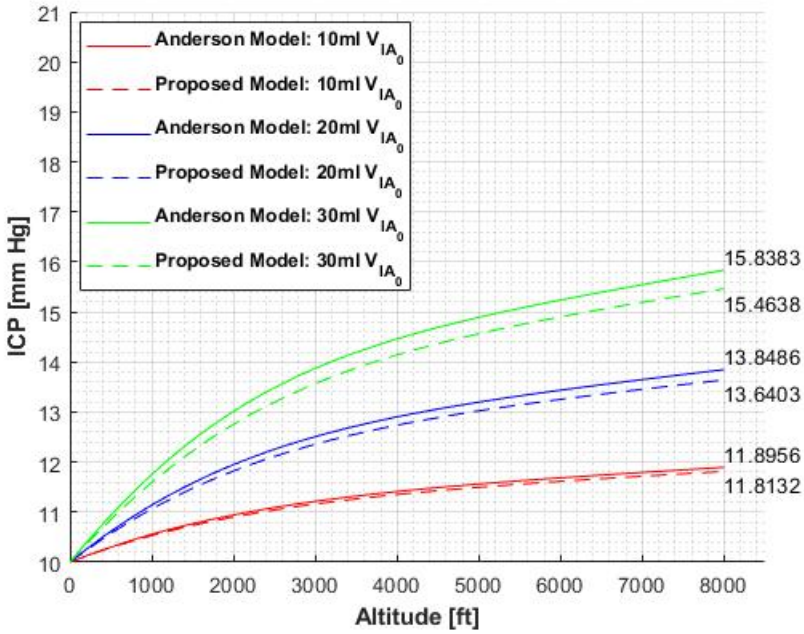

(a) 10 mm Hg

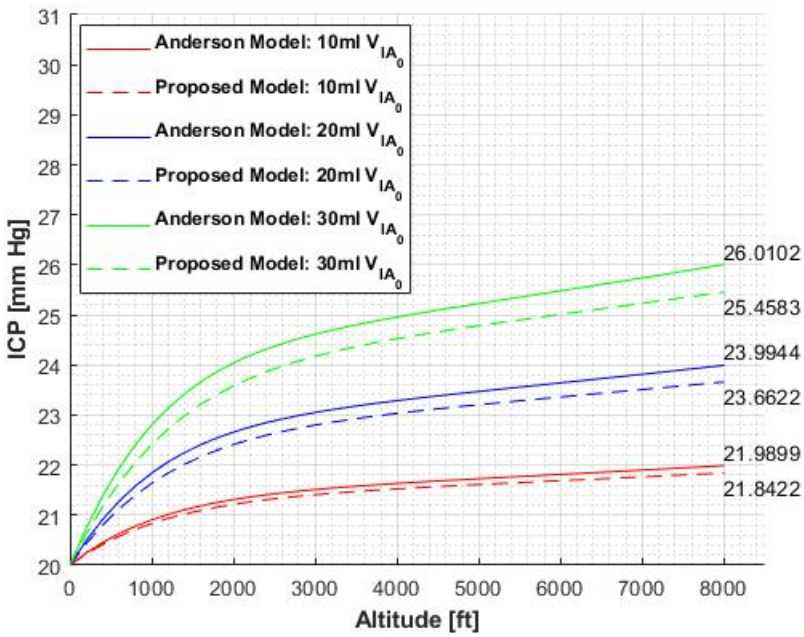

(b) 20 mm Hg

Figure A.3: Change in ICP during ascent at 250 ft·min^1, simulated for three initial volumes and two resting ICP

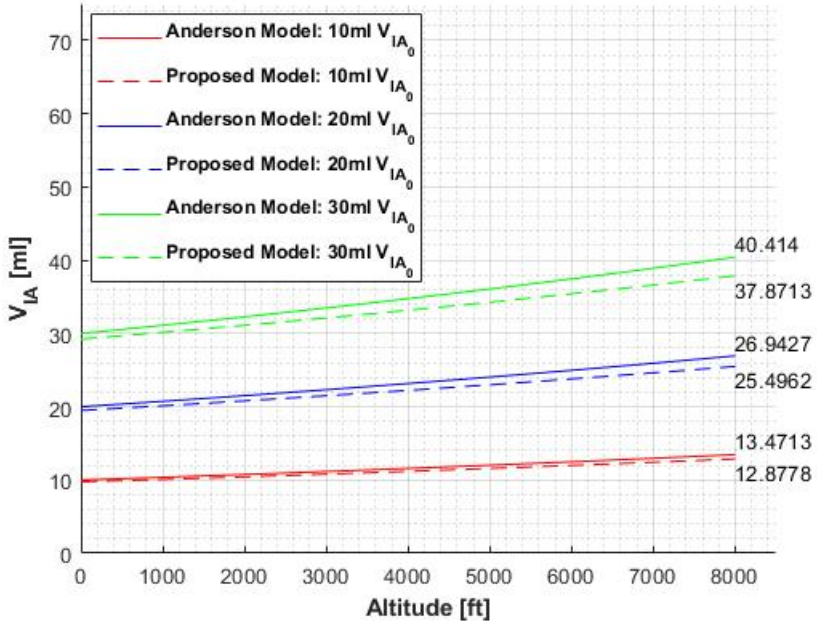

Figure A.4: Change in intracranial air volume during ascent at 1000 ft·min^1, simulated for three initial volumes

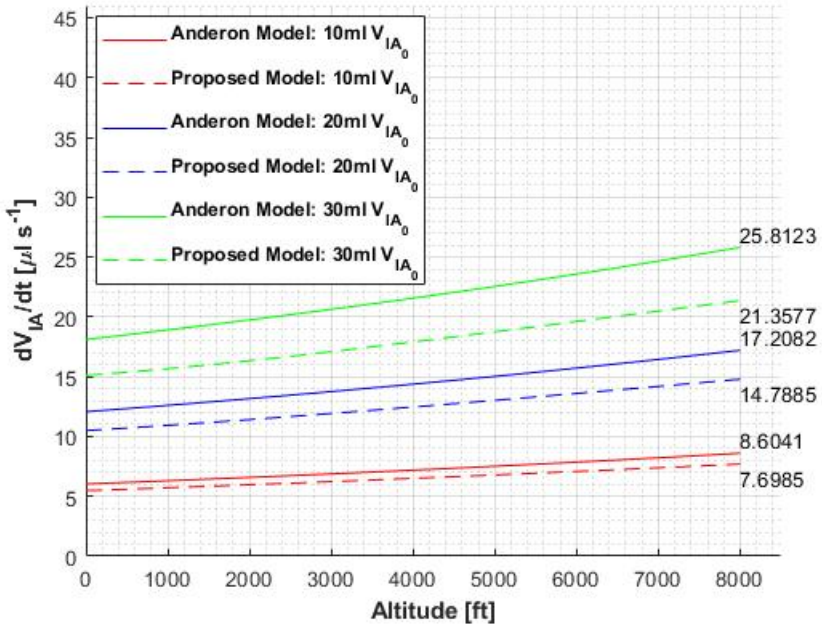

Figure A.5: Rate of change of intracranial air volume during ascent at 1000 ft·min^1, simulated for three initial volumes

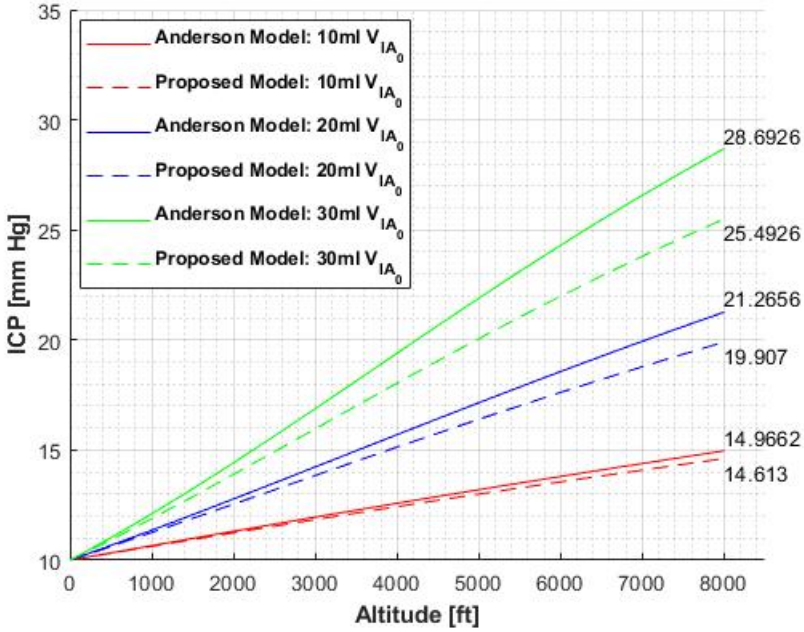

(a) 10 mm Hg

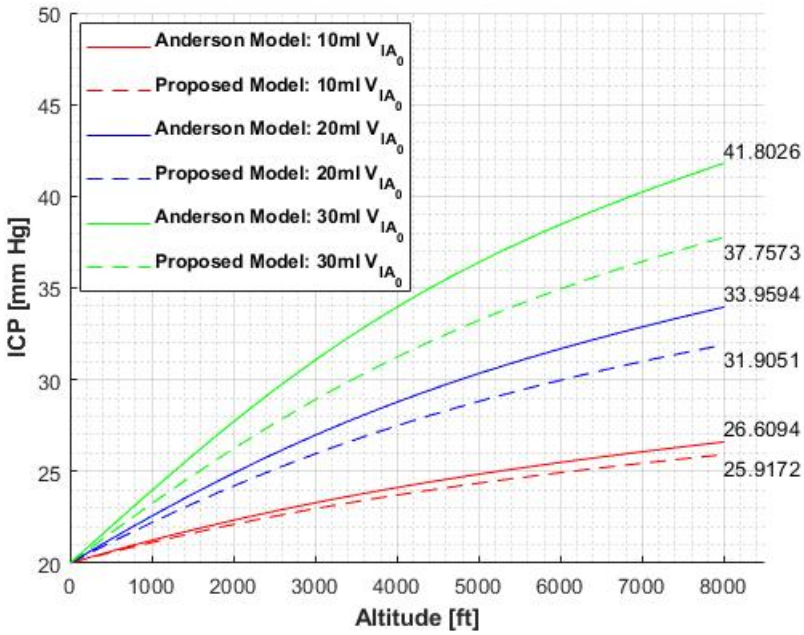

(b) 20 mm Hg

Figure A.6: Change in ICP during ascent at 1000 ft·min^1, simulated for three initial volumes and two resting ICP

A.2 Varying Ascension Rates

Simulated results for varying ascension rates are presented here.

A.2.1 Logarithmic Ascension

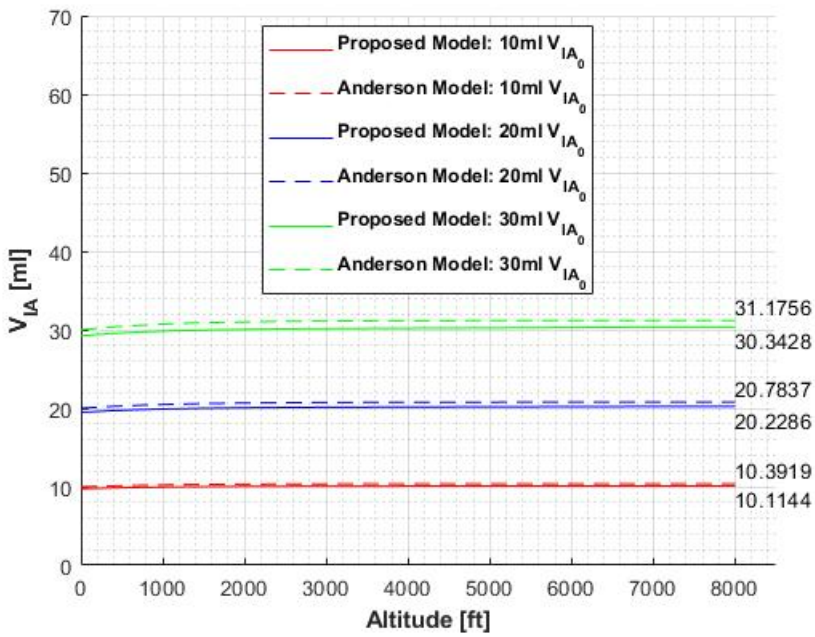

Figure A.7: Change in intracranial air volume during logarithmic ascension, simulated for three initial volumes corresponding to 250 ft·min^{-1}

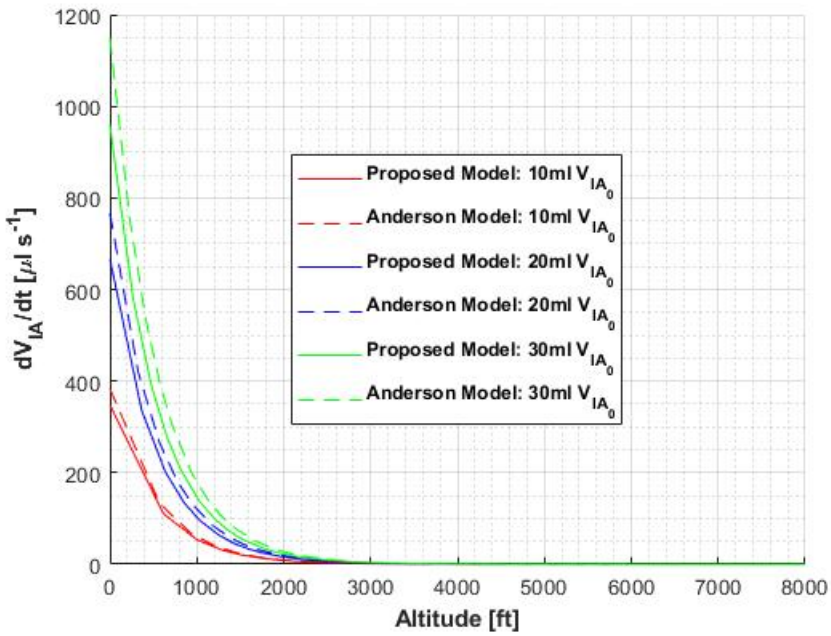

Figure A.8: Rate of change of intracranial air volume during logarithmic ascension, simulated for three initial volumes corresponding to 250 ft·min[1]

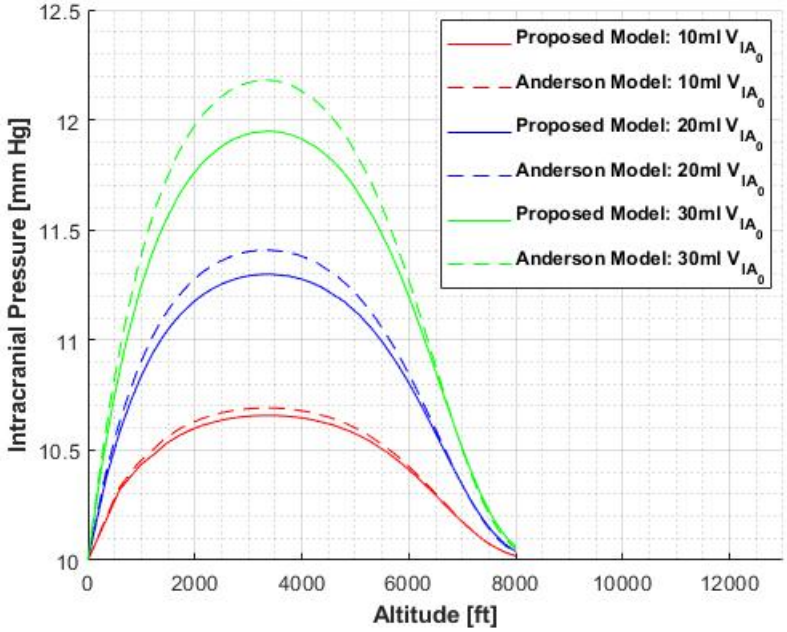

(a) 10 mm Hg

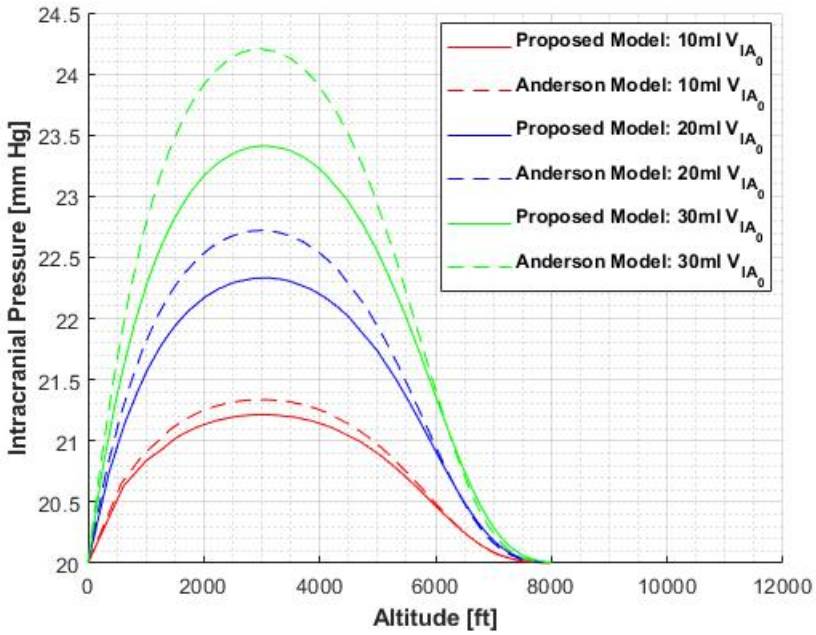

(b) 20 mm Hg

Figure A.9: Change in ICP during logarithmic ascension with three initial volumes and two resting pressures, corresponding to 250 ft·min[1]

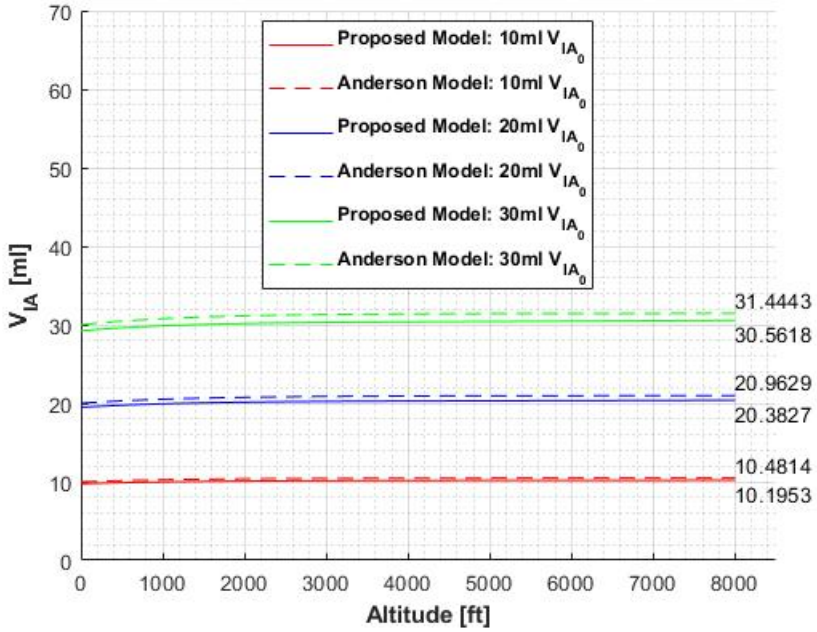

Figure A.10: Change in intracranial air volume during logarithmic ascension, simulated for three initial volumes corresponding to 1000 ft·min^{-1}

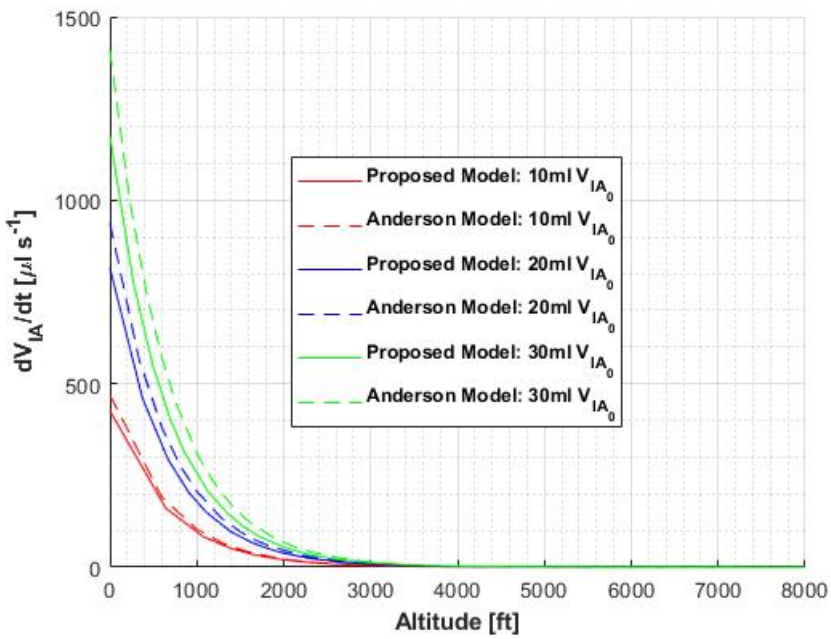

Figure A.11: Rate of change of intracranial air volume during logarithmic ascension, simulated for three initial volumes corresponding to 1000 ft·min^{1}

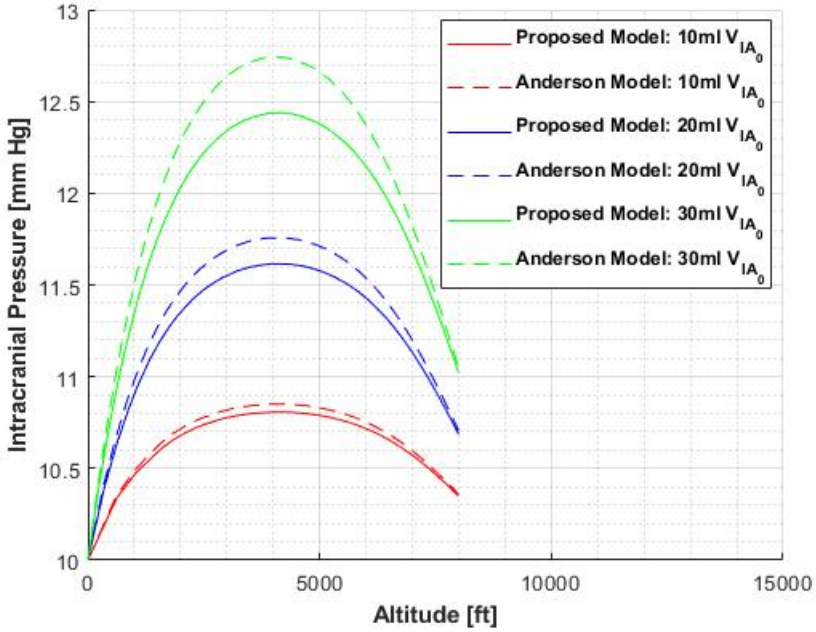

(a) 10 mm Hg

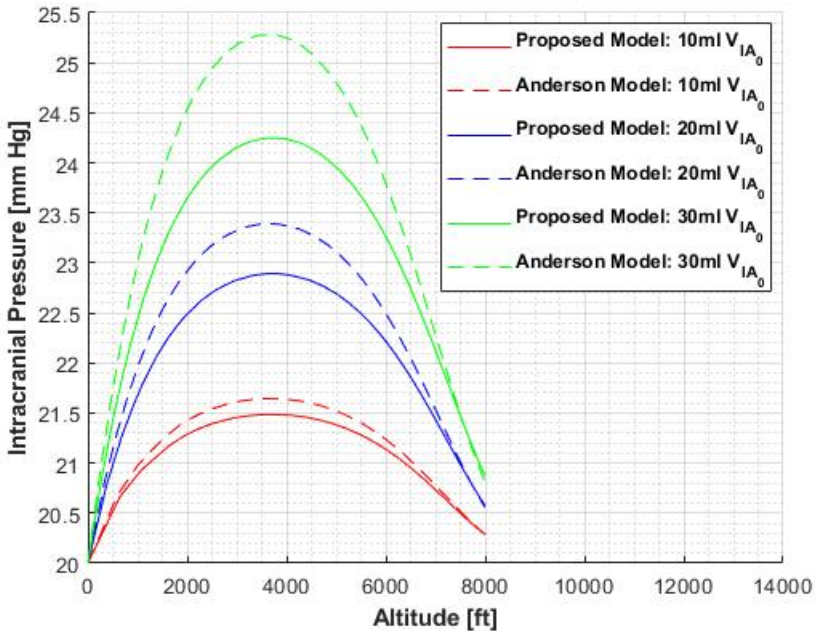

(b) 20 mm Hg

Figure A.12: Change in ICP during logarithmic ascension with three initial volumes and two resting pressures, corresponding to 1000 ft·min[1]

A.2.2 Exponential Ascension

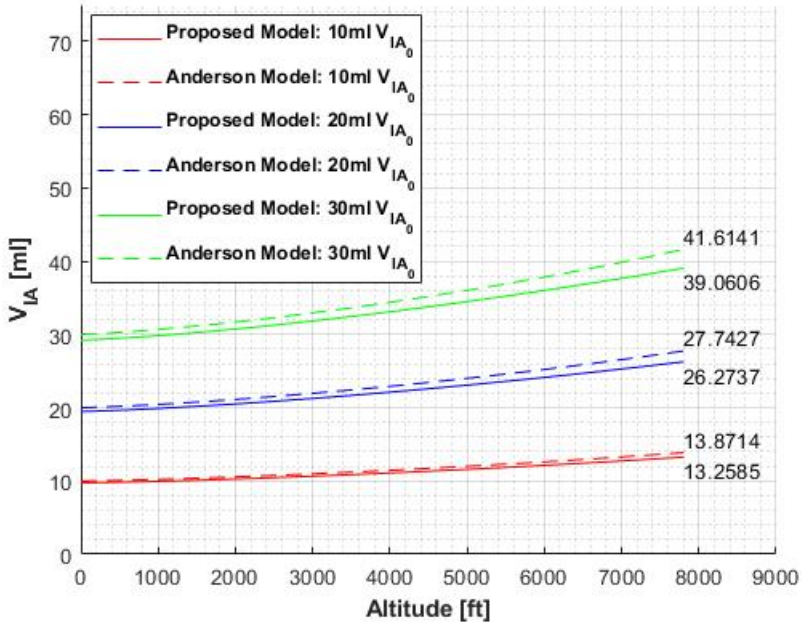

Figure A.13: Change in intracranial air volume during exponential ascension, simulated for three initial volumes corresponding to 250 ft·min^{-1}

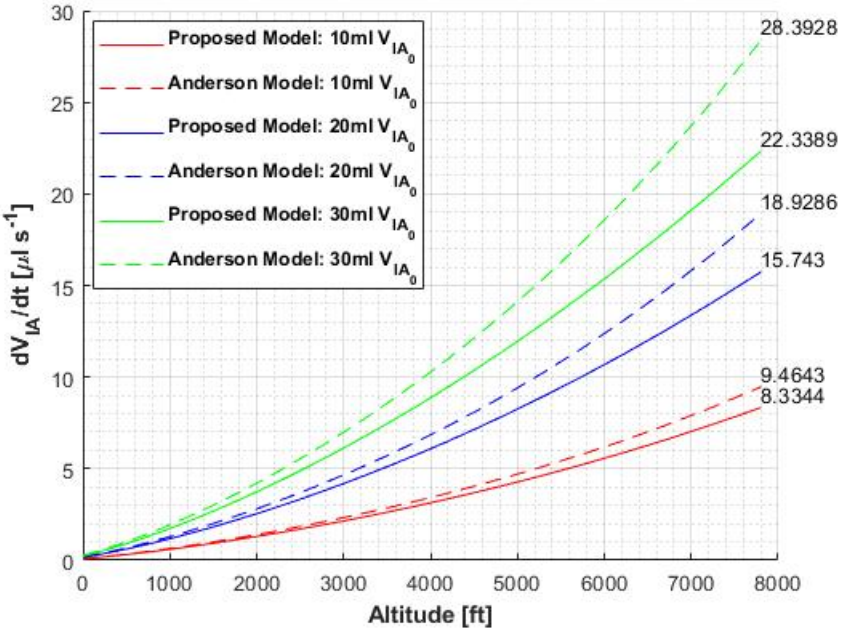

Figure A.14: Rate of change of intracranial air volume during exponential ascension, simulated for three initial volumes corresponding to 250 ft·min[1]

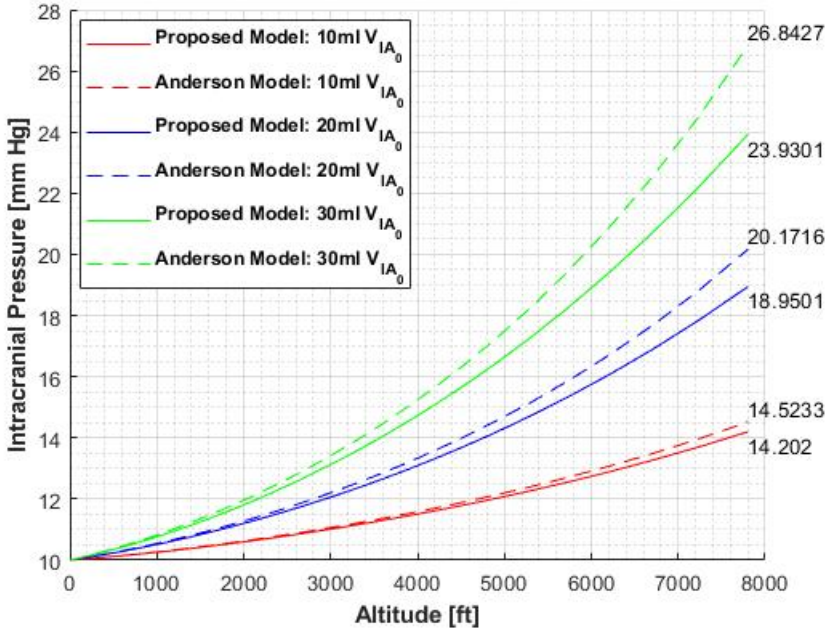

(a) 10 mm Hg

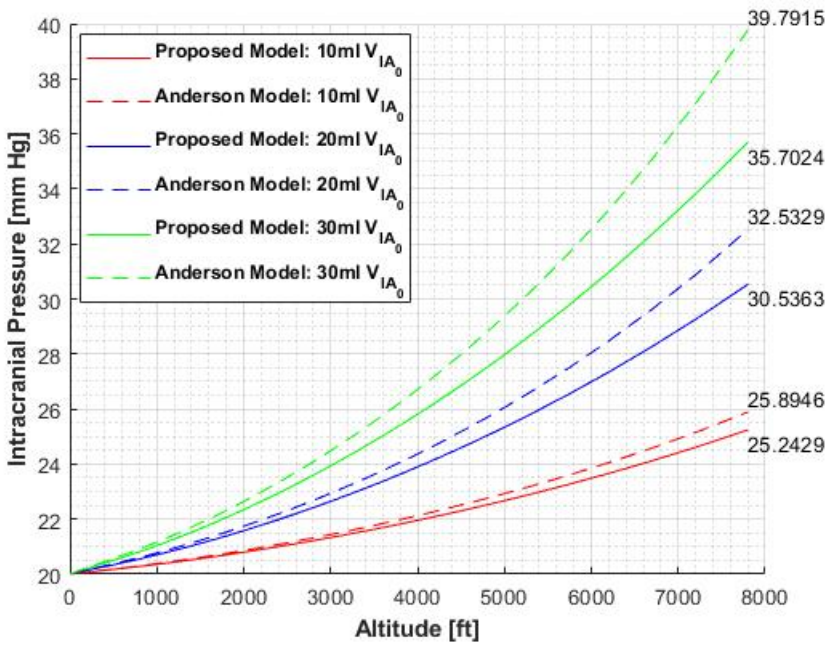

(b) 20 mm Hg

Figure A.15: Change in ICP during exponential ascension with three initial volumes and two resting pressures, corresponding to 250 ft·min[1]

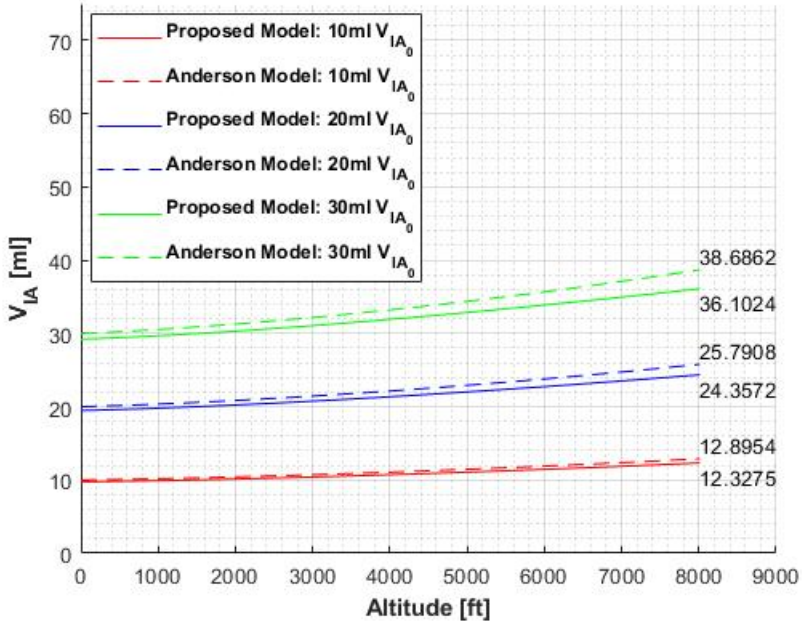

Figure A.16: Change in intracranial air volume during exponential ascension, simulated for three initial volumes corresponding to 1000 ft·min^{-1}

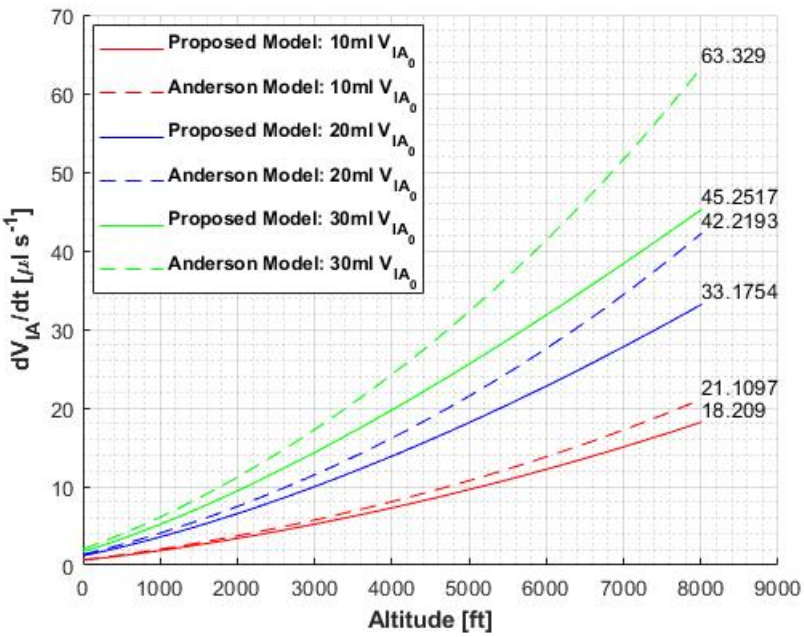

Figure A.17: Rate of change of intracranial air volume during exponential ascension, simulated for three initial volumes corresponding to 1000 ft·min^{1}

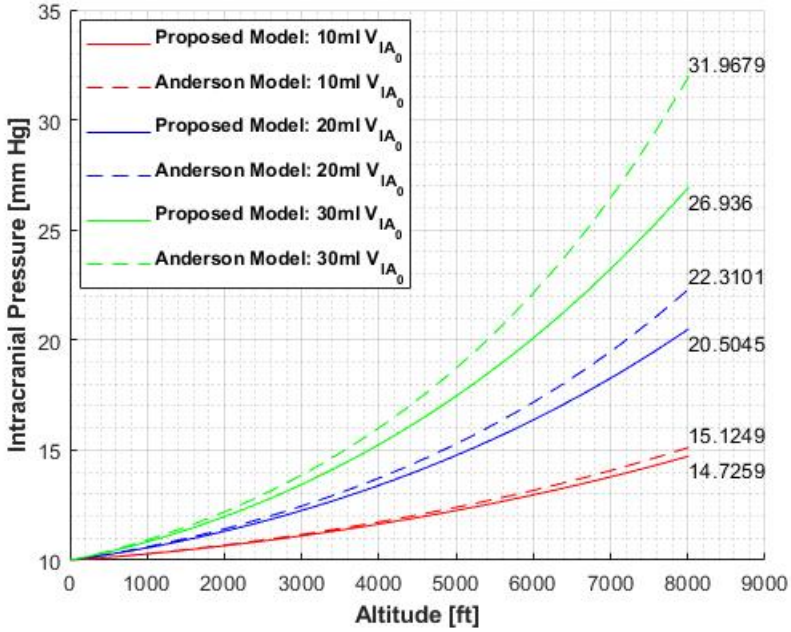

(a) 10 mm Hg

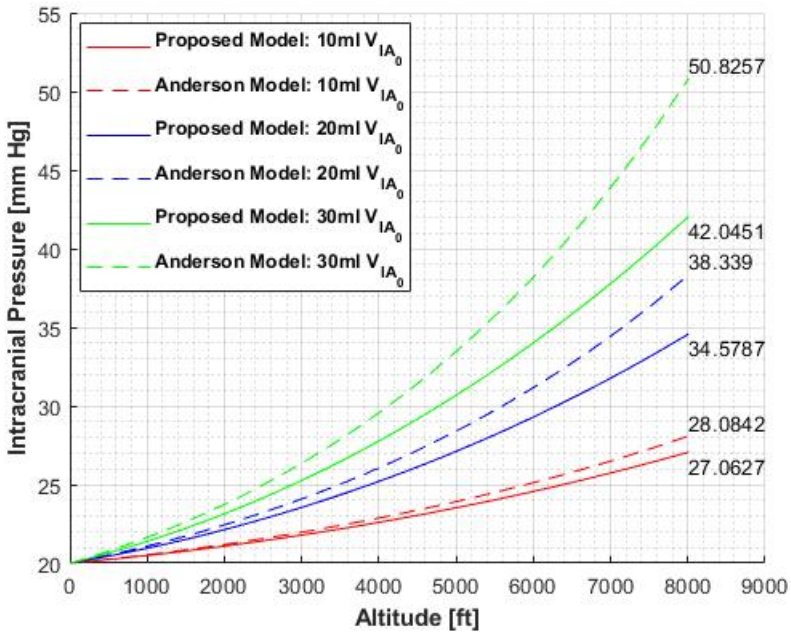

(b) 20 mm Hg

Figure A.18: Change in ICP during exponential ascension with three initial volumes and two resting pressures, corresponding to 1000 ft·min^1

Appendix B

MATLAB Code

The following sections include the codes used to run the simulations. The codes were written in MATLAB R2018b.

B.1 Constant Ascension Rates

```
% A Mathematical Modelling Study of the Effects of Air Expansion ...
    Inside the
% Brain on the Intracranial Pressure

% Monash University Malaysia - Final Year Project
% Written by Viruj BALA SOUPRAMANIEN (27273652)
% Last modified: 29/5/19

% Anderson et al. Model
% Replicating results from: Andersson et al. (2003) - Air ...
    Transport of
% Patients with Intracranial Air: Computer Model of Pressure Effects

clc; clear; close all;

```

```
% Table 2 values
PICr=[10 20]*133.322; % Resting pressure (Pa)
VICr=[150 120]*1e-6; % Resting CSF volume
PVI=12.6*1e-6; % Pressure-volume index (m^3)
R=16.1*8.0124e9; % Outflow resistance (Pa/(m^3.s))
VIA0=[10 20 30]*1e-6; % Initial intracranial volume (m^3)
dHdt=[250 500 1000]*0.3048/60; % Rate of ascension (m/s)
Hmax=8000*0.3048; % Maximum altitude (m)

% Numerical constants
a=2257e-8; % Alpha
b=5.264; % Beta
K=1/(0.4343*PVI); % Mathematical constant

for k=1:length(dHdt)
    dt(k)=Hmax/dHdt(k); % Time taken to reach 8000 ft
    for j=1:length(VIA0)
        V=@(t)VIA0(j)./(1-a.*dHdt(k).*t).^b; % Equation 13
        dVdt=@(t)a*b*VIA0(j).*dHdt(k)./((1-a.*dHdt(k).*t).^(b+1)); ...
            % Rate of change of intracranial air equation
        for i=1:length(PICr)
            dPdt=@(t,P)(K*P/R)*(PICr(i)+R*dVdt(t)-P); % Equation 8
            [t,P]=ode45(dPdt,[0 dt(k)],PICr(i)); % Solving ...
                equation 8
            H{i,j,k}=dHdt(k)*t/0.3048; % Cabin altitude (ft)
            P_IC{i,j,k}=P/133.322; % Intracranial pressure (mm Hg)
            V_IC{i,j,k}=(log(P./PICr(i))/K+VICr(i))*1e6; % ...
                Intracranial volume (ml)
            V_IA{i,j,k}=V(t)*1e6; % Intracranial air volume (ml)
            P_IA{i,j,k}=(101000*(1-a*dHdt(k).*t).^b)/133.322;
            rate{i,j,k}=dVdt(t)*1e9; % Rate of change of volume ...
                (ul/s)
        end
    end
end

% Proposed Model
% Verifying Anderson model using function of intracranial ...
    pressure [P_IC(t)]
```

```
clear A Patm dPatm l m n o t P dPdt V dV dicv icp icv iav iap ...
    delV alt;

PIA0=101e3; % Initial intracranial air pressure

for n=1:length(dHdt)
    for m=1:length(VIA0)
        for l=1:length(PICr)
            A=VIA0(m)*PIA0; % From Boyles law: P1V1=P2V2 ...
                (A=V_IA*P_IA)
            Patm=@(t)PIA0*(1-a*dHdt(n).*t).^b; % Atmospheric ...
                pressure
            dPatm=@(t)-a*b*PIA0*dHdt(n).*(1-a*dHdt(n).*t).^(b-1); ...
                % Rate of change of atmospheric pressure
            V=@(t,P)A./(Patm(t)+P);
            dPdt=@(t,P)(K*P./(R*((Patm(t)+P).^2+K*P*A))).*...
                ((PICr(l)-P).*(Patm(t)+P).^2-A*R*dPatm(t)); % ...
                    Equation 8
            dV=@(t,P)-A*(dPatm(t)+dPdt(t,P))./((Patm(t)+P).^2);
            [t,P]=ode45(dPdt,[0 dt(n)],PICr(l)); % Solving ...
                equation 8
            icp{l,m,n}=P/133.322; % Intracranial pressure (mm Hg)
            icv{l,m,n}=(log(P./PICr(l))/K+VICr(l))*1e6; % ...
                Intracranial volume (ml)
            alt{l,m,n}=dHdt(n)*t/0.3048; % Altitude (ft)
            iav{l,m,n}=V(t,P)*1e6; % Intracranial air volume (ml)
            iap{l,m,n}=(Patm(t)+P)/133.322;
            delV{l,m,n}=dV(t,P)*1e9; % Rate of change of ...
                intracranial volume (ul/s)
        end
    end
end

% Plots

if PICr(1)≠10 && VIA0(1)≠10 && dHdt(1)≠250
    PICr=PICr/133.322;
    VIA0=VIA0/1e-6;
```

```
    dHdt=dHdt*60/0.3048;
end

[u,v,w]=size(icp);
lines={'r','b','g';'rs:','bs:','gs:';'r--','b--','g--'};

for x=1:u
    for y=1:v
        if x==1
            c=1;
        else
            c=10;
        end
        for z=1:w
            figure(c)
            hold on
            plot(H{x,y,z},V_IA{x,y,z},lines{1,y},'DisplayName',...
                ['Anderson Model: ',num2str(VIA0(y)),'ml ...
                    V_{IA}_{_0}'])
            plot(alt{x,y,z},iav{x,y,z},lines{3,y},'DisplayName',...
                ['Proposed Model: ',num2str(VIA0(y)),'ml ...
                    V_{IA}_{_0}'])
            %title(sprintf('Change in Air Volume with Altitude ...
                at %d ft/min (P_{IC}_{_r} = %d mm ...
                Hg)',dHdt(z),PICr(x)))
            legend('-DynamicLegend','Location','best',...
                'FontWeight','bold')
            text(H{x,y,z}(end),V_IA{x,y,z}(end),...
                num2str(V_IA{x,y,z}(end)),'HorizontalAlignment',...
                'left','VerticalAlignment','bottom')
            text(H{x,y,z}(end),iav{x,y,z}(end),...
                num2str(iav{x,y,z}(end)),'HorizontalAlignment',...
                'left','VerticalAlignment','top')

            figure(c+1)
            hold on
            plot(H{x,y,z},rate{x,y,z},lines{1,y},'DisplayName',...
                ['Anderon Model: ',num2str(VIA0(y)),'ml ...
                    V_{IA}_{_0}'])
```

```
            plot(alt{x,y,z},delV{x,y,z},lines{3,y},'DisplayName',...
                ['Proposed Model: ',num2str(VIA0(y)),'ml ...
                    V_{IA}_{_0}'])
            %title(sprintf('Rate of Air Expansion against ...
                Altitude at %d ft/min (P_{IC}_{_r} = %d mm ...
                Hg)',dHdt(z),PICr(x)))
            legend('-DynamicLegend','Location','best',...
                'FontWeight','bold')
            text(H{x,y,z}(end),rate{x,y,z}(end),...
                num2str(rate{x,y,z}(end)),'HorizontalAlignment',...
                'left','VerticalAlignment','bottom')
            text(H{x,y,z}(end),delV{x,y,z}(end),...
                num2str(delV{x,y,z}(end)),'HorizontalAlignment',...
                'left','VerticalAlignment','top')

            figure(c+2)
            hold on
            plot(H{x,y,z},P_IC{x,y,z},lines{1,y},'DisplayName',...
                ['Anderson Model: ',num2str(VIA0(y)),'ml ...
                    V_{IA}_{_0}'])
            plot(alt{x,y,z},icp{x,y,z},lines{3,y},'DisplayName',...
                ['Proposed Model: ',num2str(VIA0(y)),'ml ...
                    V_{IA}_{_0}'])
            %title(sprintf('Change in ICP with Altitude at %d ...
                ft/min (P_{IC}_{_r} = %d mm Hg)',dHdt(z),PICr(x)))
            legend('-DynamicLegend','Location','best',...
                'FontWeight','bold')
            text(H{x,y,z}(end),P_IC{x,y,z}(end),...
                num2str(P_IC{x,y,z}(end)),'HorizontalAlignment',...
                'left','VerticalAlignment','bottom')
            text(H{x,y,z}(end),icp{x,y,z}(end),...
                num2str(icp{x,y,z}(end)),'HorizontalAlignment',...
                'left','VerticalAlignment','top')

            % Cleaning up presentation
            if z==1
                figure(c)
                axis([0 8500 0 75])
                figure(c+1)
```

```
                axis([0 8500 0 12])
                if x==1
                    figure(c+2)
                    axis([0 8500 10 21])
                else
                    figure(c+2)
                    axis([0 8500 20 31])
                end
            elseif z==2
                figure(c)
                axis([0 8500 0 75])
                figure(c+1)
                axis([0 8500 0 25])
                if x==1
                    figure(c+2)
                    axis([0 8500 10 26])
                else
                    figure(c+2)
                    axis([0 8500 20 40])
                end
            else
                figure(c)
                axis([0 8500 0 75])
                figure(c+1)
                axis([0 8500 0 46])
                if x==1
                    figure(c+2)
                    axis([0 8500 10 35])
                else
                    figure(c+2)
                    axis([0 8500 20 50])
                end
            end

            figure(c)
            xlabel('Altitude [ft]','FontWeight','bold')
            ylabel('V_{IA} [ml]','FontWeight','bold')
            grid on
            grid minor
```

```
            figure(c+1)
            xlabel('Altitude [ft]','FontWeight','bold')
            ylabel('{dV_{IA}}/{dt} [\mul ...
                s^{-1}]','FontWeight','bold')
            grid on
            grid minor
            figure(c+2)
            xlabel('Altitude [ft]','FontWeight','bold')
            ylabel('ICP [mm Hg]','FontWeight','bold')
            grid on
            grid minor
            c=c+3;
        end
    end
end
```

B.2 Varying Ascension Rates

```
% A Mathematical Modelling Study of the Effects of Air Expansion ...
    Inside the
% Brain on the Intracranial Pressure

% Monash University Malaysia - Final Year Project
% Written by Viruj BALA SOUPRAMANIEN (27273652)
% Last modified: 10/9/19

% Change in ICP when change in altitude follows exponential and ...
    logarithmic
% functions

clc; clear all; close all;

% Logarithmic

% Table 2 values
PICr=[10 20]*133.322; % Resting pressure (Pa)
```

```
PVI=12.6*1e-6; % Pressure-volume index (m^3)
R=16.1*8.0124e9; % Outflow resistance (Pa/(m^3.s))
VIA0=[10 20 30]*1e-6; % Initial intracranial volume (m^3)
dt=[32 16 8]*60; % Time to reach maximum altitude (s)

% Numerical constants
a=2257e-8; % Alpha
b=5.264; % Beta
K=1/(0.4343*PVI); % Mathematical constant
PIA0=101e3; % Absolute initial intracranial air (Pa) = P_atm at ...
    sea level

% Log function coefficients
X=[322.514 355.0392 394.8271];

for n=1:length(X)
    for m=1:length(VIA0)
        for l=1:length(PICr)
            A=VIA0(m)*PIA0; % From Boyles Law: P1V1=P2V2 ...
                (A=V_IA*P_IA)
            Patm=@(t)PIA0*(1-a*X(n).*t./(t+1)).^b; % Atmospheric ...
                pressure
            dPatm=@(t)-a*b*PIA0*(X(n)./(t+1)-X(n).*...
                t./(t+1).^2).*(1-a*X(n).*t./(t+1)).^(b-1); % ...
                    Rate of change of atmospheric pressure
            V=@(t,P)A./(Patm(t)+P); % Intracranial air volume
            dPdt=@(t,P)(K*P./(R*((Patm(t)+P).^2+K*P*A))).*...
                ((PICr(l)-P).*(Patm(t)+P).^2-A*R*dPatm(t)); % ...
                    Equation 8
            dV=@(t,P)-A*(dPatm(t)+dPdt(t,P))./((Patm(t)+P).^2);
            [t,P]=ode45(dPdt,[0 dt(n)],PICr(l)); % Solving ...
                equation 8
            icp{l,m,n}=P/133.322; % Intracranial pressure (mm Hg)
            alt{l,m,n}=X(n)*log(t+1)/0.3048; % Altitude (ft)
            iav{l,m,n}=V(t,P)*1e6; % Intracranial air volume (ml)
            delV{l,m,n}=dV(t,P)*1e9; % Rate of change of ...
                intracranial volume (ul/s)
            time{l,m,n}=t/60; % Time taken to reach 8000 ft (min)
            % Anderson Model
```

```
            V_Anderson=@(t)A./Patm(t); % Intracranial air volume
            dV_Anderson=@(t)-A*dPatm(t)./((Patm(t)).^2);
            dPdt_Anderson=@(t,P)(K*P/R)*(PICr(l)...
                +R*dV_Anderson(t)-P); % Equation 8
            [t,P]=ode45(dPdt_Anderson,[0 dt(n)],PICr(l)); % ...
                Solving equation 8
            P_IC{l,m,n}=P/133.322; % Intracranial pressure (mm Hg)
            H{l,m,n}=X(n)*log(t+1)/0.3048; % Altitude (ft)
            V_IA{l,m,n}=V_Anderson(t)*1e6; % Intracranial air ...
                volume (ml)
            rate{l,m,n}=dV_Anderson(t)*1e9; % Rate of change of ...
                intracranial volume (ul/s)
        end
    end
end

% Plots

[u,v,w]=size(icp);
PICr=PICr/133.322;
VIA0=VIA0/1e-6;
X=[2288 2824 3641];
lines={'r','b','g';'r--','b--','g--'};

for x=1:u
    for y=1:v
        if x==1
            c=1;
        else
            c=10;
        end
        for z=1:w
            figure(c)
            hold on
            plot(alt{x,y,z},iav{x,y,z},lines{1,y},'DisplayName',...
                ['Proposed Model: ',num2str(VIA0(y)),'ml ...
                    V_{IA}_{_0}'])
            plot(H{x,y,z},V_IA{x,y,z},lines{2,y},'DisplayName',...
```

```
                ['Anderson Model: ',num2str(VIA0(y)),'ml ...
                    V_{IA}_{_0}'])
            %title(sprintf('Change in Air Volume with Change in ...
                Altitude of %s*log(t+1) ft (P_{IC}_{_r} = %s mm ...
                Hg)',num2str(X(z)),num2str(PICr(x))))
            text(H{x,y,z}(end),V_IA{x,y,z}(end),...
                num2str(V_IA{x,y,z}(end)),'HorizontalAlignment',...
                'left','VerticalAlignment','bottom')
            text(H{x,y,z}(end),iav{x,y,z}(end),...
                num2str(iav{x,y,z}(end)),'HorizontalAlignment',...
                'left','VerticalAlignment','top')

            figure(c+1)
            hold on
            plot(alt{x,y,z},delV{x,y,z},lines{1,y},'DisplayName',...
                ['Proposed Model: ',num2str(VIA0(y)),'ml ...
                    V_{IA}_{_0}'])
            plot(H{x,y,z},rate{x,y,z},lines{2,y},'DisplayName',...
                ['Anderson Model: ',num2str(VIA0(y)),'ml ...
                    V_{IA}_{_0}'])
            %title(sprintf('Rate of Air Expansion against Change ...
                in Altitude of %s*log(t+1) ft (P_{IC}_{_r} = %s ...
                mm Hg)',num2str(X(z)),num2str(PICr(x))))

            figure(c+2)
            hold on
            plot(alt{x,y,z},icp{x,y,z},lines{1,y},'DisplayName',...
                ['Proposed Model: ',num2str(VIA0(y)),'ml ...
                    V_{IA}_{_0}'])
            plot(H{x,y,z},P_IC{x,y,z},lines{2,y},'DisplayName',...
                ['Anderson Model: ',num2str(VIA0(y)),'ml ...
                    V_{IA}_{_0}'])
            %title(sprintf('Change in ICP with Change in ...
                Altitude of %s*log(t+1) ft (P_{IC}_{_r} = %s mm ...
                Hg)',num2str(X(z)),num2str(PICr(x))))

            % Cleaning up presentation
            if z==1
                figure(c)
```

```
                axis([0 8500 0 70])
                if x==1
                    figure(c+2)
                    axis([0 13000 10 12.5])
                else
                    figure(c+2)
                    axis([0 12000 20 24.5])
                end
            elseif z==2
                figure(c)
                axis([0 8500 0 70])
                if x==1
                    figure(c+2)
                    axis([0 14000 10 12.5])
                else
                    figure(c+2)
                    axis([0 14000 20 25])
                end
            else
                figure(c)
                axis([0 8500 0 70])
                if x==1
                    figure(c+2)
                    axis([0 15000 10 13])
                else
                    figure(c+2)
                    axis([0 14000 20 25.5])
                end
            end

            figure(c)
            xlabel('Altitude [ft]','Fontweight','bold')
            ylabel('V_{IA} [ml]','Fontweight','bold')
            legend('-DynamicLegend','Location','best',...
                'Fontweight','bold')
            grid on
            grid minor
            figure(c+1)
            xlabel('Altitude [ft]','Fontweight','bold')
```

```
            ylabel('{dV_{IA}}/{dt} [\mul ...
                s^{-1}]','Fontweight','bold')
            legend('-DynamicLegend','Location','best',...
                'Fontweight','bold')
            grid on
            grid minor
            figure(c+2)
            xlabel('Altitude [ft]','Fontweight','bold')
            ylabel('Intracranial Pressure [mm ...
                Hg]','Fontweight','bold')
            legend('-DynamicLegend','Location','best',...
                'Fontweight','bold')
            grid on
            grid minor
            c=c+3;
        end
    end
end

% Exponential

PICr=PICr*133.322;
VIA0=VIA0*1e-6;

% Exp function coefficients
Y=[141.49 223.042 375.228];
Z=[0.0015 0.0026 0.0042];

for n=1:length(Y)
    for m=1:length(VIA0)
        for l=1:length(PICr)
            A=VIA0(m)*PIA0; % From Boyles Law: P1V1=P2V2 ...
                (A=V_IA*P_IA)
            Patm=@(t)PIA0*(1-a*Y(n)*Z(n).*...
                (exp(Z(n).*t-1)).*t).^b; % Atmospheric pressure
            dPatm=@(t)-a*b*PIA0*(Y(n)*Z(n).*...
                (exp(Z(n).*t-1))+Y(n)*Z(n).^2.*...
                (exp(Z(n).*t-1)).*t).*(1-a*Y(n)*...
```

```
                Z(n).*(exp(Z(n).*t-1)).*t).^(b-1); % Rate of ...
                    change of atmospheric pressure
            V=@(t,P)A./(Patm(t)+P); % Intracranial air volume
            dPdt=@(t,P)(K*P./(R*((Patm(t)+P).^2+K*P*A))).*...
                ((PICr(l)-P).*(Patm(t)+P).^2-A*R*dPatm(t)); % ...
                    Equation 8
            dV=@(t,P)-A*(dPatm(t)+dPdt(t,P))./((Patm(t)+P).^2);
            [t,P]=ode45(dPdt,[0 dt(n)],PICr(l)); % Solving ...
                equation 8
            icp{l,m,n}=P/133.322; % Intracranial pressure (mm Hg)
            alt{l,m,n}=Y(n).*(exp(Z(n).*t)-1)/0.3048; % Altitude ...
                (ft)
            iav{l,m,n}=V(t,P)*1e6; % Intracranial air volume (ml)
            delV{l,m,n}=dV(t,P)*1e9; % Rate of change of ...
                intracranial volume (ul/s)
            time{l,m,n}=t/60; % Time taken to reach 8000 ft (min)
            % Anderson Model
            V_Anderson=@(t)A./Patm(t); % Intracranial air volume
            dV_Anderson=@(t)-A*dPatm(t)./((Patm(t)).^2);
            dPdt_Anderson=@(t,P)(K*P/R)*(PICr(l)+...
                R*dV_Anderson(t)-P); % Equation 8
            [t,P]=ode45(dPdt_Anderson,[0 dt(n)],PICr(l)); % ...
                Solving equation 8
            P_IC{l,m,n}=P/133.322; % Intracranial pressure (mm Hg)
            H{l,m,n}=Y(n).*(exp(Z(n).*t)-1)/0.3048; % Altitude (ft)
            V_IA{l,m,n}=V_Anderson(t)*1e6; % Intracranial air ...
                volume (ml)
            rate{l,m,n}=dV_Anderson(t)*1e9; % Rate of change of ...
                intracranial volume (ul/s)
        end
    end
end

% Plots

PICr=PICr/133.322;
VIA0=VIA0/1e-6;
Y=[464 732 1231];
Z=[0.09 0.16 0.25];
```

```
for x=1:u
    for y=1:v
        if x==1
            c=19;
        else
            c=29;
        end
        for z=1:w
            figure(c)
            hold on
            plot(alt{x,y,z},iav{x,y,z},lines{1,y},'DisplayName',...
                ['Proposed Model: ',num2str(VIA0(y)),'ml ...
                    V_{IA}_{_0}'])
            plot(H{x,y,z},V_IA{x,y,z},lines{2,y},'DisplayName',...
                ['Anderson Model: ',num2str(VIA0(y)),'ml ...
                    V_{IA}_{_0}'])
            title(sprintf('Change in Air Volume with Change in ...
                Altitude of %s*exp(%s*t-1) ft (P_{IC}_{_r} = %s ...
                mm ...
                Hg)',num2str(Y(z)),num2str(Z(z)),num2str(PICr(x))))
            text(H{x,y,z}(end),V_IA{x,y,z}(end),...
                num2str(V_IA{x,y,z}(end)),'HorizontalAlignment',...
                'left','VerticalAlignment','bottom')
            text(H{x,y,z}(end),iav{x,y,z}(end),...
                num2str(iav{x,y,z}(end)),'HorizontalAlignment',...
                'left','VerticalAlignment','top')

            figure(c+1)
            hold on
            plot(alt{x,y,z},delV{x,y,z},lines{1,y},'DisplayName',...
                ['Proposed Model: ',num2str(VIA0(y)),'ml ...
                    V_{IA}_{_0}'])
            plot(H{x,y,z},rate{x,y,z},lines{2,y},'DisplayName',...
                ['Anderson Model: ',num2str(VIA0(y)),'ml ...
                    V_{IA}_{_0}'])
            title(sprintf('Rate of Air Expansion against Change ...
                in Altitude of %s*exp(%s*t+1) ft (P_{IC}_{_r} = ...
                %s mm ...
```

```
                Hg)',num2str(Y(z)),num2str(Z(z)),num2str(PICr(x))))
            text(H{x,y,z}(end),rate{x,y,z}(end),...
                num2str(rate{x,y,z}(end)),'HorizontalAlignment',...
                'left','VerticalAlignment','bottom')
            text(H{x,y,z}(end),delV{x,y,z}(end),...
                num2str(delV{x,y,z}(end)),'HorizontalAlignment',...
                'left','VerticalAlignment','bottom')

            figure(c+2)
            hold on
            plot(alt{x,y,z},icp{x,y,z},lines{1,y},'DisplayName',...
                ['Proposed Model: ',num2str(VIA0(y)),'ml ...
                    V_{IA}_{_0}'])
            plot(H{x,y,z},P_IC{x,y,z},lines{2,y},'DisplayName',...
                ['Anderson Model: ',num2str(VIA0(y)),'ml ...
                    V_{IA}_{_0}'])
            title(sprintf('Change in ICP with Change in Altitude ...
                of %s*exp(%s*t+1) ft (P_{IC}_{_r} = %s mm ...
                Hg)',num2str(Y(z)),num2str(Z(z)),num2str(PICr(x))))
            text(H{x,y,z}(end),P_IC{x,y,z}(end),...
                num2str(P_IC{x,y,z}(end)),'HorizontalAlignment',...
                'left','VerticalAlignment','bottom')
            text(H{x,y,z}(end),icp{x,y,z}(end),...
                num2str(icp{x,y,z}(end)),'HorizontalAlignment',...
                'left','VerticalAlignment','top')

            % Cleaning up presentation
            if z==1
                figure(c)
                axis([0 9000 0 75])
            elseif z==2
                figure(c)
                axis([0 9000 0 75])
            else
                figure(c)
                axis([0 9000 0 75])
            end

            figure(c)
```

```
            xlabel('Altitude [ft]','Fontweight','bold')
            ylabel('V_{IA} [ml]','Fontweight','bold')
            legend('-DynamicLegend','Location','best',...
                'Fontweight','bold')
            grid on
            grid minor
            figure(c+1)
            xlabel('Altitude [ft]','Fontweight','bold')
            ylabel('{dV_{IA}}/{dt} [\mul ...
                s^{-1}]','Fontweight','bold')
            legend('-DynamicLegend','Location','best',...
                'Fontweight','bold')
            grid on
            grid minor
            figure(c+2)
            xlabel('Altitude [ft]','Fontweight','bold')
            ylabel('Intracranial Pressure [mm ...
                Hg]','Fontweight','bold')
            legend('-DynamicLegend','Location','best',...
                'Fontweight','bold')
            grid on
            grid minor
            c=c+3;
        end
    end
end
```

B.3 Temperature Effect

```
% A Mathematical Modelling Study of the Effects of Air Expansion ...
    Inside the
% Brain on the Intracranial Pressure

% Monash University Malaysia - Final Year Project
% Written by Viruj BALA SOUPRAMANIEN (27273652)
% Last modified: 29/9/19
```

```
% Effects of temperature on intracranial system with pneumocephalus

clc; clearvars -except dy; close all;

% Parameters
PICr=[10 20]*133.322; % Resting intracranial pressure (Pa)
PVI=12.6*1e-6; % Pressure-volume index (m^3)
R=16.1*8.0124e9; % Outflow resistance (Pa/(m^3.s))
VIA0=[10 20 30]*1e-6; % Initial intracranial volume (m^3)
Ti=[18 21 24]+273.15; % Initial body temperature (K)
dt=[5 8 15]; % Time taken to reach final body temperature (s)

% Mathematical constant
K=1/(0.4343*PVI);

% Coefficients
grad=[3.5394 2.9728 2.4502;2.3215 1.953 1.58125;...
    1.250733333 1.052533333 0.854733333];
C=[Ti;Ti;Ti];

for n=1:length(Ti)
    for m=1:length(VIA0)
        Temp=@(t)grad(m,n)*t+C(m,n);
        dT=grad(m,n);
        CL(m,n)=VIA0(m)./Ti(n); % From Charles Law: V1/T1=V2/T2 ...
            (A=V_IA/T_f) (m^3/K)
        dVdt=CL(m,n).*dT; % Rate of change of intracranial air ...
            volume (m^3/s)
        for l=1:length(PICr)
            dPdt=@(t,P)(K*P/R)*(PICr(l)+R*dVdt-P); % Equation 8
            [t,P]=ode45(dPdt,[0 dt(m)],PICr(l)); % Solving ...
                equation 8
            icp{l,m,n}=P/133.322; % Intracranial pressure (mm Hg)
        end
        iav{m,n}=CL(m,n).*Temp(t)*1e6; % Intracranial air volume ...
            (ml)
        T{m,n}=Temp(t)-273.15; % Body temperature (C)
        time{m,n}=t; % Time taken (s)
```

```
        delV{m,n}=dVdt*1e9; % Rate of change of intracranial air ...
            volume (ul/s)
    end
end


[u,v,w]=size(icp);
PICr=PICr/133.322;
VIA0=VIA0/1e-6;
Ti=Ti-273.15;
lines={'r','b','g';'r--','b--','g--';'r.','b.','g.'};

for x=1:u
    for y=1:v
        for z=1:w
            if x==1
                if z==1
                    c=1;
                elseif z==2
                    c=3;
                else
                    c=5;
                end
                figure(c)
                hold on
                plot(T{y,z},iav{y,z},lines{1,y},'DisplayName',...
                    ['V_{IA}_{0} = ',num2str(VIA0(y)),'ml'])
                legend('-DynamicLegend','Location','best'...
                    ,'FontWeight','bold')
                xlabel('Temperature [\circC]','FontWeight','bold')
                ylabel('V_{IA} [ml]','FontWeight','bold')
                grid on
                grid minor
                text(T{y,z}(end),iav{y,z}(end),...
                    num2str(iav{y,z}(end)),'HorizontalAlignment',...
                    'left','VerticalAlignment','bottom')
            else
                if z==1
                    c=6;
```

```
                elseif z==2
                    c=7;
                else
                    c=8;
                end
            end
            figure(c+1)
            hold on
            plot(T{y,z},icp{x,y,z},lines{1,y},'DisplayName',...
                ['V_{IA}_{0} = ',num2str(VIA0(y)),'ml'])
            %title(sprintf('Change in ICP with Change in ...
                Temperature (P_{IC}_{_r} = %s mm ...
                Hg)',num2str(PICr(x))))
            text(T{y,z}(end),icp{x,y,z}(end),...
                num2str(icp{x,y,z}(end)),'HorizontalAlignment',...
                'left','VerticalAlignment','bottom')
            legend('-DynamicLegend','Location','best'...
                ,'FontWeight','bold')
            xlabel('Temperature [\circC]','FontWeight','bold')
            ylabel('Intracranial Pressure [mm ...
                Hg]','FontWeight','bold')
            grid on
            grid minor
            c=c+2;
        end
    end
end
```

Appendix C

Reflections on Program Outcomes (PO) Achievement

Program Outcomes	Reflections
PO1 **Mechanical Engineering Knowledge:** Apply knowledge of mathematics, natural science, engineering fundamentals and specialisation in Mechanical engineering to the solution of complex engineering problems	Sound scientific method and research practices were applied
PO2 **Problem Analysis:** Identify, formulate, survey research literature and analyze complex Mechanical engineering problems reaching substantiated conclusions using first principles of mathematics, natural sciences and engineering sciences	Research plan based on scientific methodologies and research practices
PO3 **Design/Development of Solutions:** Design solutions for complex Mechanical engineering problems and design systems, components or processes that meet specified needs.	Formulated solutions from existing knowledge and skills
PO4 **Research-based Investigation:** Conduct investigations of complex Mechanical engineering problems using research-based knowledge and research methods including design of experiments, (analysis and interpretation of data, and synthesis of information to provide valid conclusions.	Independently conducted scientific based research under broad directions. Justified validity of project and pointed out limitations by applying techniques of scientific theory to provide logical reasoning
PO5 **Modern Tool Usage:** Create, select and apply appropriate techniques, resources, and modern engineering and IT tools, including prediction and modelling, to complex Mechanical engineering problems, with an understanding of the limitations	MATLAB and Monash library services used for project
PO6 **Engineer and Society:** Apply reasoning informed by contextual knowledge to assess societal, health, safety, legal and cultural issues and the consequent responsibilities relevant to professional engineering practice and solutions to complex Mechanical engineering problems	Solution to real-world problem sought through project
PO7 **Environment and Sustainability:** Understand and evaluate the sustainability and impact of professional engineering work in the solution of complex Mechanical engineering problems in environmental contexts.	N/A

PO8 **Ethics:** Apply ethical principles and commit to professional ethics and responsibilities and norms of engineering practice.	Ethical principles in research conduct and academic writing
PO9 **Communication:** Communicate effectively on complex Mechanical engineering activities with the engineering community and with society at large, such as being able to comprehend and write effective reports and design documentation, make effective presentations, and give and receive clear instructions	Communicated findings to professional audience and community at large through academic writing and oral presentation
PO10 **Individual and Teamwork:** Function effectively as an individual, and as a member or leader in diverse teams and in multi-disciplinary settings	Functioned effectively individually with guidance of supervisor
PO11 **Lifelong Learning:** Recognise the need for, and have the preparation and ability to engage in independent and life-long learning in the broadest context of technological change	Review and critical analysis of scientific literature relevant to the research
PO12 **Project Management and Finance:** Demonstrate knowledge and understanding of engineering management principles and economic decision-making and apply these to manage projects	Managed project effectively within technical, risk and time constraint

Appendix D

Seminar Attendance Sheets

MEC4401 S1 2019 Seminar Attendance Sheet

Name: Viraj Bala Soupramanien

Student ID: 27273662

***Attendance to all seminars is compulsory and the speakers' signatures are proof of your attendance. Please obtain signature from the speaker at the end of each session.*

Date	Seminar	Speaker	Signature
06 Mar 19	**FYP briefing**	Dr Ooi Ean Hin	
20 Mar 19	Literature Review workshop	Ms Aini Fatimah	
21 Mar 19	Effective Searching workshop	~~Ms Nur Muzzamil~~ Belinda	
27 Mar 19	Risk Assessment workshop	Mr Jasbir	
4 Apr 19	Managing References with EndNote	~~Ms Nur Muzzamil~~ Belinda	
11 Apr 19	Seminar by Professional Engineer	Ir Lee Chang Quan	
17 Apr 19	Technical writing workshop	A/P Hung Yew Mun	

Note: Please keep this attendance sheet with you until the end of the semester. This sheet must be attached to your thesis at the last page prior to binding

MEC4402 S2 2019 Seminar Attendance Sheet

Name: Viraj Bala Sayramanian

Student ID: 27273652

**Attendance to all seminars is compulsory and the speakers' signatures are proof of your attendance. Please obtain signature from the speaker at the end of each session.

Date	Seminar	Speaker	Signature
1 August 2019	FYP Briefing	Dr. Foo Ji Jinn	
8 August 2019	MS report formatting	Ms. Belinda.sta.maria	
21 August 2019	Data Analysis Workshop	Dr. Arshad Salema	
28 August 2019	Research Paper and Thesis Writing Workshop	Dr. Arshad Salema	
5 September 2019	Seminar by Professional Engineer	Ir. Choo CM	
19 September 2019	Presentation skills workshop	Mr. Esmael Yahaya	

Note: Please keep this attendance sheet with you until the end of the semester. This sheet must be attached to your thesis at the last page prior to binding